Antemortem Diagnostics in Prion Disease

by

Danielle Gushue

A thesis submitted in partial fulfillment of the requirements for the degree of

Master of Science

in

Animal Science

Department of Agricultural, Food and Nutritional Science
University of Alberta

Abstract

Antemortem identification of Creutzfeldt-Jakob disease (CJD) patients is initially based upon clinical presentation of the disease. Symptoms are assessed in combination with results from cerebrospinal fluid (CSF) analysis, electroencephalography (EEG), magnetic resonance imaging (MRI), and real-time quaking-induced conversion assay (RT-QuIC) for diagnostic purposes. Inconsistencies in sensitivities and specificities of prion disease biomarker abundance in CSF have been described and a lack of standardization for how biomarker levels are measured has been identified. Clinical presentation and progression of human prion disease is variable due to factors such as prion protein genotype, prion strain and other undefined genetic or environmental contributions, which may confound the appearance or abundance of biomarkers. By contrast, prion disease in laboratory rodents follows a defined disease course as the infection route and time, prion strain, genotype and environmental conditions are all controlled. We adapted prion disease to rats, facilitating a proteomic approach to a bioavailable fluid, CSF, at preclinical and clinical disease stages. This contrasts with human CJD samples, which are generally only available at clinical stage. The rat CSF proteome was compared between infected rats and age-matched controls through mass spectrometry. A number of proteins up-regulated and/or specific to prion disease were identified. These proteins included known CJD biomarkers, 14-3-3 and neuron-specific enolase (NSE), demonstrating the utility of using rat prion disease for biomarker identification. The objective of this study is to validate the use of these markers at clinical stage and to define the pre-clinical abundance, as the utility of 14-3-3 and NSE at pre-clinical disease stages are not well characterized. Tracking the progression of prion infection in rats will allow us to further define prion disease neurodegeneration and will allow for identification of novel

biomarker candidates that may offer greater utility at both pre-clinical and clinical stages as diagnostic and prognostic tools.

Preface

The research project, of which this thesis is a part, received research ethics approval from the University of Alberta Research Ethics Board, Project Name “Etiology and Pathogenesis of Prion Diseases”, AUP00000914. Some of the research conducted for this thesis resulted from an international research collaboration with Dr. Lingjun Li at the University of Wisconsin-Madison. The literature review in Chapter 1, data analysis in Chapters 2 and 3, as well as Chapter 4 “Conclusions and Future Directions” are my original work. Dr. Allen Herbst and I were responsible for the data collection in Chapters 2 and 3 and Dr. Herbst contributed to manuscript edits. Dr. Judd Aiken, Dr. Debbie McKenzie, and Dr. Valerie Sim were the supervisory authors and were involved with concept formation and manuscript composition. Parts of Chapters 2 and 3 are in preparation for manuscript publication.

To Sang Gyun, who taught me to trust my hands and raise my hair.

Acknowledgments

I would like to thank my supervisor, Dr. Judd Aiken, for his guidance, patience, and encouragement throughout this journey, and whose enthusiasm inspired me to keep questioning. I would also like to thank my thesis supervisory committee members, Dr. Debbie McKenzie, Dr. Valerie Sim, and Dr. Leluo Guan for their helpful comments and suggestions that have allowed me to develop my work and kick it up a notch.

I would like to express my gratitude to the Aiken/McKenzie lab, past and present, for your invaluable teachings, friendships, and for creating a positive learning environment. Thank you to Dr. Allen Herbst for taking me under his wing for this project and pushing me to ask deeper questions and expand my knowledge in this field. Thank you to Dr. Debbie McKenzie for her guidance and helping me to develop my writing skills.

I would like to thank my parents, Donna and Ron who have been by my side every step of the way and who probably know my project as well as I do. Without their love and encouragement, none of this would be possible. Thank you to my brother Colin, and the rest of my family and friends for their endless love and support. Most of all, thank you to Tim for never doubting.

Table of Contents

List of Tables

List of Figures

Glossary of Terms

CJD - Creutzfeldt-Jakob disease

CSF – Cerebrospinal fluid

EEG - Electroencephalography

MRI - Magnetic resonance imaging

RT-QuIC - Real-time quaking-induced conversion

NSE - Neuron-specific enolase

TSE - Transmissible spongiform encephalopathy

PrP^{c} - Cellular prion protein

PrP^{Sc} - Infectious prion protein

CNS - Central nervous system

BSE - Bovine spongiform encephalopathy

CWD - Chronic Wasting Disease

sCJD - Sporadic Creutzfeldt-Jakob disease

PK - Proteinase K

WHO - World Health Organization

gCJD - Genetic Creutzfeldt-Jakob disease

GSS - Gerstmann-Straussler-Scheinker

FFI - Fatal familial insomnia

iCJD - iatrogenic Creutzfeldt-Jakob disease

vCJD - variant Creutzfeldt-Jakob disease

PSWCs - Periodic sharp wave complexes

DWI - Diffusion-weighted imaging

FLAIR - Fluid-attenuated inversion recovery

PMCA - Protein misfolding cyclic amplification

GPI - Glycosylphosphatidylinositol

PrP^{Res} - Protease resistant prion protein

PrP^{Sen} - Protease sensitive prion protein

recPrP - Recombinant prion protein

ThT-Thioflavin T

IHC - Immunohistochemistry

RLN - Retropharyngeal lymph nodes

RAMALT - Rectoanal mucosa-associated lymphoid tissue

RML - Name of mouse-adapted scrapie strain

RAS - Rat-adapted scrapie

DPI - Days post inoculation

ELISA - Enzyme linked immunosorbent assay

ROC - Receiver operating characteristic

AUC - Area under the curve

RMP - Reference measurement procedures

Chapter 1: Prion Disease Diagnostics

1.1 Prion Diseases

Prion diseases, or transmissible spongiform encephalopathies (TSEs), are a group of infectious, neurodegenerative disorders that affect humans and other mammals. Prion diseases are always fatal and are characterized by an extended preclinical, asymptomatic period followed by a rapid clinical phase. Prion diseases arise when the normal cellular prion protein (PrP^{C}) is converted into infectious protease-resistant aggregates, PrP^{Sc}, through a process where the α-helical structure and coil structure is refolded into β-sheet[1, 2]. This misfolded particle has been given the term 'prion', for its proteinaceous and infectious nature[3]. Through histopathological findings, TSEs can be characterized by spongiform degeneration, reactive astrocytosis, and the accumulation of fibrillary amyloid plaques in the central nervous system (CNS)[4]. Human prion diseases such as Creutzfeldt-Jakob disease (CJD) and Kuru have been identified[5]. Prion diseases affect other mammals, including sheep (scrapie), cattle (bovine spongiform encephalopathy (BSE)), and cervids (chronic wasting disease (CWD)) [2, 6]. Definitive diagnosis is typically performed post-mortem, at the end-stage of disease. There is a necessity for highly sensitive and specific antemortem techniques that will aid in the diagnosis and prognosis of prion infection.

1.2 Human Prion Diseases

Human prion diseases can be categorized aetiologically into three classes: sporadic, genetic, and acquired. These classifications are further divided based on molecular features[7].

1.2.1 Sporadic CJD

The human prion disease, sporadic CJD (sCJD) was first described by Hans Gerhard Creutzfeldt and Alfons Maria Jakob in the early 1920's[3]. sCJD accounts for greater than 80% of CJD cases; the rate of occurrence is approximately one case per million per year worldwide[3]. The cause of sCJD remains unknown. It has been hypothesized that sCJD may result from the horizontal transmission of prions from humans or animals, from somatic mutation of the PrP gene, or spontaneous conversion of PrP^{C} to PrP^{Sc} [3]. Codon 129 on the prion protein gene (*PRNP*) is the site of a common polymorphism that impacts CJD susceptibility and involves methionine (M)/ Valine (V). Possible genotypes are MM or VV homozygous, or MV heterozygous at codon 129. There are two types of PrP^{Sc} associated with human prion diseases: PrP^{Sc} type 1 and PrP^{Sc} type 2, which are distinguishable based on size and resistance to proteinase K (PK) digestion which is observed on Western blots[8, 9]. The electrophoretic profile of protease resistant PrP^{Sc}

unglycosylated fragments in sCJD are observed at 21kDa (type 1) or 19kDa (type 2)[10-13]. Six molecular type classifications are determined based on codon 129 polymorphisms and PrP^{Sc} type: MM1, MM2, MV1, MV2, VV1, and VV2 (Figure 1-1)[14]. These six types do not necessarily display unique clinical and pathological differences, but can be further classified based on other features, for example: pathology, prevalence, age of onset, disease duration, and clinical presentation (Table 1-1)[14, 15]. Clinicians characterize sCJD according to World Health Organization (WHO) standards based on presentation of symptoms and biomarker indicators to classify patients as having possible or probable sCJD [16]. Definite sCJD is determined via post-mortem analysis of the diseased brain (Figure 1-1).

1.2.2 Genetic CJD

Genetic CJD is associated with autosomal dominant genetic polymorphisms of the *PRNP* gene and accounts for 10-15% of CJD cases[7, 17]. More than 50 mutations in the open reading frame of *PRNP* have been described[18]. There is variability in the clinical and pathological findings, age of onset, and disease duration which can also depend on the codon 129 polymorphism[17, 19, 20]. Genetic CJD can be further categorized into three phenotypes: genetic Creutzfeldt-Jakob disease (gCJD), Gerstmann-Straussler-Scheinker disease (GSS), and fatal familial insomnia (FFI) (Figure 1-1). Genetic CJD can be caused by point or insertional mutations including E200K and V210I[18]. E200K and V210I mutation carriers typically demonstrate clinical and pathological features similar to sCJD (MM1) cases where the average age of clinical onset is between 50 and 70 years and disease duration is typically less than six months[18]. The most common mutation for GSS occurs at codon 102 (P102L)[18]. GSS is associated with prominent ataxia and dementia tends to set in at the late stage of disease with disease duration is between 1 and 7 years[18]. GSS histopathology reveals large PrP-amyloid plaques in the molecular layer of the cerebellum and spongiform changes are often missing[18]. FFI is the most common genetic prion disease worldwide[18]. Early symptoms include sleep and vigilance disturbances, cognitive deficits, spatial disorientation, hallucinations, autonomic disturbances, and motoric signs[18]. Disease duration for FFI ranges between 6 and 72 months[18]. The duration of illness for genetic prion diseases is often extended when compared to sCJD, where clinical stage may last for several years[19].

1.2.3 Acquired CJD

The acquired form of CJD is distinguishable from sCJD by early age of onset, absence of electroencephalography (EEG) changes typically found in CJD and presence of distinct neuro-pathological features[17]. Acquired CJD affects <1% of the global population. Transmission is either oral through contaminated food products or iatrogenic via surgical instruments, and tissue transplants[21]. Three forms of acquired CJD have been identified; Kuru, iatrogenic CJD (iCJD), and variant CJD (vCJD) (Figure 1-1).

Kuru was first identified in the Fore people of Papua, New Guinea by Gajdusek and colleagues in 1957, and is the result of ritualistic cannibalism[5,22,23]. Neuropathology of Kuru is characterized by amyloid plaques, astroglial and microglial proliferation, and spongiosis of the diseased brain[24]. In 1959, William Hadlow proposed that scrapie infection observed in sheep was similar to that observed in Kuru patients and had the potential to also be infectious[25]. Animal bioassays were performed and Kuru was the first human neurodegenerative disease found to be infectious via transmission into chimpanzees in 1966, followed by the transmission of CJD into chimpanzees in 1968[23,26]. Further investigation in Kuru-affected areas led to conclusions that MM homozygous was the more susceptible genotype and had an earlier age of disease onset and a relatively short incubation period in comparison to the late disease onset with a long incubation period observed in MV and VV genotypes [27].

Persons at risk of iatrogenic CJD include recipients of human tissue derived pituitary hormone treatment (either growth hormone or gonadotrophin), dura mater grafts (until 1992 for Lyodura grafts, until 1997 for Tutoplast Dura grafts), corneal grafts, or patients who have been exposed, via contact with instruments, to high-infectivity tissue of confirmed CJD patients, as summarized by the Public Health Agency of Canada[28,29]. Use of sources such as cadaver-sourced pituitary growth hormone were prohibited in 1985 in the UK, iatrogenic CJD continues to be problematic in this area. One study that investigated growth hormone induced iatrogenic transmission of CJD in the years 2000-2014, found the frequency of cases that continue to be identified fall between 0-6 cases per year in the UK [30]. Furthermore, an extended incubation period of 18-40 years was observed in these cases. In Canada, there have been four reported cases associated with dura mater grafts, and no corneal graft or human growth hormone associated CJD reports[29].

Variant CJD is the result of an exposure to BSE prions[31]. There have been 178 cases reported in the UK, and an additional 54 cases worldwide in 11 different countries, with 2 reported in Canada (as of July 2016)[32, 33]. It has been hypothesized that a portion of the UK population could still be incubating vCJD with a possibility for secondary vCJD cases via blood or tissue donations and surgical instrument contamination[34]. A study of archived appendix samples investigated the prevalence of subclinical prion infection. The study characterized samples from 1941-60 and 1961-85 birth cohorts, as well as samples removed from 2000-2012[35] and identified an estimated prevalence of 1 in 2000 people to be carriers, suggesting that a second wave of subclinical carriers have not been detected in the population[35]. Furthermore, iatrogenic transmission of vCJD has been demonstrated by three secondary vCJD cases that have been linked to blood transfusions, where one blood donation was made more than 3 years prior to the donor became symptomatic for vCJD[34, 36]. The possibility of a population acting as silent carriers underlies the importance of epidemiological surveillance systems and the need for pre-clinical, antemortem testing[31, 35].

1.3 Detecting Prion Diseases

Historically, detection of prion infection relied on histopathology, identification of spongiform degeneration, combined with animal bioassay. While definitive determination of prion infection is performed post-mortem, emphasis has been placed on antemortem detection to gain further understanding into the pathobiology of prion infection at preclinical and clinical stages, to investigate therapeutic intervention, and to mitigate risk of transmission.

1.3.1 Current Ante-mortem Methods for CJD Diagnosis

1.3.1.1 Biopsy

The gold standard for definitive diagnosis of CJD is the histopathological examination of brain biopsies, or occasionally tonsil for suspected vCJD cases[37]. Testing is performed during the clinical stage of disease. Although this technique can be utilized for confirmatory diagnosis, the procedure is highly invasive. Diagnosis in the clinical phase of disease combined with the invasiveness and risk associated with this technique emphasizes the need for earlier and more practical testing. Analysis of the diseased brain is generally only performed via post-mortem autopsy[37].

1.3.1.2 Electroencephalography (EEG)

EEG can be used for the ante-mortem diagnosis of CJD. In sCJD, a disease-specific pattern is displayed, where periodic sharp wave complexes (PSWCs) consisting of triphasic waves at 1-2 Hz can be observed[17]. These characteristic EEG patterns are only observed in the later stages of the disease. Furthermore this test demonstrates variable sensitivity (65-85%) and can be occasionally observed in other neurodegenerative disorders[38-41]. Age of onset and disease duration may also have an impact on sensitivity[42]. EEG analysis demonstrates lower sensitivity and specificity in genetic and acquired prion diseases, including vCJD, when compared to sCJD cases[43-46].

1.3.1.3 Magnetic Resonance Imaging (MRI)

Initially MRI played a minimal role in the clinical diagnosis of CJD, and was primarily used for differential diagnosis to exclude other explanations for brain damage such as stroke (ischemic or hemorrhagic), multiple sclerosis, hydrocephalus, tumors, or chronic meningoencephalitis[47, 48]. Hyper-intensities have been found to correlate with the location of vacuolation and PrP^{Sc} deposition and can be used to distinguish strains and sCJD molecular subtypes[39, 49]. In 2009, it was reported that the basal ganglia and cortical hyper-intensities represent the most frequent MRI findings in sCJD and are present in most cases[50]. Diffusion-weighted imaging (DWI) provides image contrast based on differences in the magnitude of diffusion of water molecules within the brain[51]. Fluid-attenuated inversion recovery (FLAIR) imaging suppresses CSF signal[52]. Combining both DWI and FLAIR imaging allows for 91% sensitivity, 95% specificity, and 94% accuracy in differentiating CJD from other dementias[39]. It was proposed that MRI be added to the WHO diagnostic criteria of sCJD in 2009[39, 50, 53, 54]. MRI has proven to have greater sensitivity and specificity than EEG and current cerebrospinal fluid (CSF) biomarkers[42, 55-57]. One key challenge with this technique is the accuracy and skill of the individual performing this procedure. Improper data acquisition and display technique as well as the susceptibility and motion artifacts may substantially impair interpretation and impact diagnosis[39].

1.4 Comparison of PrP^{Sc} detection with surrogate marker detection

1.4.1 Detection of PrP^{Sc}

As confirmatory diagnostic testing is performed post-mortem, it is important to develop ante-mortem testing strategies that are less invasive. PrP^{Sc} is present in accessible tissues or body

fluids such as blood, urine, saliva, and CSF. One infectious prion is roughly the equivalent to $<10^2$ aggregated PrP^{Sc} molecules, making direct detection of infectious prion protein challenging, as protein levels in these bio-fluids are lower than the threshold of detection of most immunoassays[58]. Methods of amplification such as protein misfolding cyclic amplification (PMCA) and Real-time quaking-induced conversion (RT-QuIC) make it possible to detect low levels of PrP^{Res}.

PMCA is a rapid and flexible *in vitro* PrP^{Sc} amplification technology that is used to detect PrP^{Sc} in tissues and biofluids using conventional assays such as western blot. The substrate used is naturally occurring PrP^{C} that is glycosylated and contains glycosylphosphatidylinositol (GPI) anchor[59, 60]. PMCA exploits the natural ability of PrP^{Sc} to convert PrP^{C} into protease-resistant aggregates. Samples undergo cycles of sonication and incubation with PrP^{Sc} template-dependent conversion[61]. PMCA can be used to model aspects of prion replication relevant to human prion disease, such as the influence of PrP^{Sc} type, *PRNP* polymorphisms, and transmission barriers[59]. Unfortunately PMCA analysis has the potential to be confounded by *de novo* generation of PrP^{Res} via off-target amplification of normal, non-infectious material[62]. In addition, novel PrP^{Sc} isoforms with unique biochemical properties may exhibit increased sensitivity to PK digestion (PrP^{Sen}). Therefore, a second limitation of PMCA is that the amount of PrP^{Sc} detected may not be representative of the infectivity being observed[63].

RT-QuIC is also a seeded prion protein conversion assay. In contrast to PMCA, RT-QuIC assay utilizes recombinant prion protein (recPrP) as the substrate instead of PrP^{C}. Recombinant PrP is purified, bacterially expressed PrP, devoid of glycans and GPI anchor, and has been through a cycle of denaturation and refolding during purification[24]. Conformational change is initiated in recPrP after seeding with PrP^{Sc} material and undergoing periodic shaking instead of sonication[59,49,64, 53]. The result is amyloid formation of recPrP that binds with thioflavin T (ThT), which is used to produce fluorescence. The fluorescence is measured using a spectrofluorometer and monitored over time[59, 65-67]. It has been shown that vCJD samples were considerably slower at seeding than sCJD samples; these differences are have been attributed to molecular properties or different proportions of recPrP that are sensitive to PK digestion[25, 59, 68]. While the positive detection of PrP^{Res} establishes a positive diagnosis of prion infection, negative results cannot confirm the absence of prion infection[58]. In CSF samples, <80% sensitivity and 100% specificity

for sCJD has been reported using this method[67, 69, 70], with some studies reporting as high as 100% sensitivity[70]. RT-QuIC has recently been added to diagnostic criteria for applications in health care settings, in conjunction with other known biomarkers to optimize both sensitivity and specificity[66, 70, 71]. Currently, use of this technology is limited to diagnostic applications in clinical stage of disease[71].

1.4.2 Indirect Detection Using CSF Surrogate Markers

CSF surrogate markers of CJD infection are tools that are used in combination with other techniques to rule out other disorders and increase certainty of diagnosis. With the discovery that proteins 130 and 131 belong to 14-3-3 family of proteins, a pre-mortem immunoassay of CSF from humans and animals with TSE was developed[72]. Presence of 14-3-3 proteins in CSF was reported as a potential biomarker for TSE's, and was added to the WHO diagnostic criteria for sporadic CJD (sCJD) in 1998[16, 72, 73]. 14-3-3s are 28-30kDa proteins present in all eukaryotic cells, and make up nearly 1% of all soluble brain proteins[74-77]. There are 7 isoforms of 14-3-3 that form cytosolic dimers[78]. Beta (β) and gamma (γ) isoforms are biomarkers in the pre-mortem diagnosis of human prion diseases, specifically sCJD[79]. The 14-3-3 proteins are not specific markers for prion disease but indicate rapid neuronal loss and are found in other neurological diseases[80]. A secondary biomarker that has been commonly reported in CJD diagnostics is neuron-specific enolase (NSE)[81]. NSE is a dimer formed in neurons and neuroendocrine tissues with isoforms, α-γ and γ-γ[82-85]. Increased concentration of 14-3-3 or NSE proteins in CSF elevates the diagnostic certainty from possible (typical clinical presentation) to probable (typical clinical presentation with additional confirmatory test results) CJD[86, 87]. Other proteins that have been reported to be elevated in CSF in sCJD patients include S-100B, and Tau protein[88]. S100B is produced by astrocytes, microglial cells and oligodendroglial cells[89, 90]. This protein acts as a stimulator of cell proliferation and migration, and inhibits apoptosis and differentiation[91]. Tau proteins are microtubule-associated proteins involved with microtubule-assembly and stabilization[92]. Abnormal modifications are associated with many neurodegenerative diseases[93]. Importantly, none of these proteins are not prion disease specific and may be representative of CNS damage and neuronal death[58]. Sensitivity and specificity can be highly variable and may be influenced by factors including age at onset, stage of illness when the sample was collected, as well as the form of CJD; in vCJD for example, protein sensitivities are much lower (25%-60%)[88]. The importance and limitations of surrogate markers for prion infection will be further

discussed in Chapter 2. Through the combination of tests including EEG, MRI, CSF testing, and clinical presentation, a multimodal approach can be taken to determine a possible or probable diagnosis of CJD that can be made with increasing certainty [50, 58, 80].

1.5 Diagnostics in Other Mammals

In sheep and goats, clinical signs of prion infection include pruritus, weight loss, wool pulling, difficulty standing, body tremor, heightened sensitivity to sounds and movement, and other abnormal behaviors[6]. BSE affected cattle may show changes in temperament such as nervousness or aggression, abnormal posture, lack of coordination, trouble standing, and weight loss[6]. The signs for CWD in cervids can include emaciation, excessive salivation, ataxia, drooping head and ears, weakness, and behavioral changes[6]. These signs are not specific enough to confirm a diagnosis of prion disease. Definitive diagnosis is achieved through post-mortem analysis of the diseased brain and is demonstrated through resistance of the prion protein to PK digestion[6].

Scrapie is a TSE with a worldwide distribution and has been endemic for over 250 years in Britain and Europe[94]. Management strategies involve eradicating diseased animals as well as populations with highly susceptible genotypes, and breeding programs are in place to promote less susceptible genotypes[94]. These strategies are now used in combination with preclinical, antemortem testing for PrP^{Sc} using immunohistochemistry (IHC) staining of lymphoid biopsy samples from tonsil, third eyelid, and rectal mucosa[94].

CWD is a prion disease in both farmed and free-ranging cervids (e.g. elk, deer, and moose). The spreading of this disease across 24 U.S. states, 2 Canadian provinces, the republic of Korea, and the recent discovery of the disease in moose and reindeer in Norway, brings CWD to the forefront of diagnostics and surveillance[95-97]. Tissues such as the obex and medial retropharyngeal lymph nodes (RLN) offer high sensitivity and specificity in IHC analysis, however, these tissues can only be collected post-mortem, causing surveillance and individual screening to be limited[98]. Alternatively, PrP^{Sc} accumulates in lymphoid tissues during the long pre-clinical stage. Biopsy of lymphoid tissues from the palatine tonsil, third eyelid, rectoanal mucosa-associated lymphoid tissue (RAMALT), and nasal brush samples collected from olfactory epithelium can be used for pre-clinical, ante-mortem diagnostics, where PrP^{Sc} is detectable through IHC immunolabelling techniques[99, 100].

RT-QuIC has been applied to diagnose sheep scrapie, rodent-adapted scrapie, and CWD[101]. Recently, a study investigated the use of RT-QuIC on RAMALT biopsy samples and nasal brushings on CWD cervids[98]. RT-QuIC used on RAMALT samples revealed 79.6% sensitivity and 100% specificity, which is similar to results observed in IHC testing[98]. Unfortunately, sensitivity for nasal brushings was reportedly very low[98]. Culling costs, costs of implementing live testing, animal welfare management, food safety, trade restrictions, and maintenance of genetic diversity are dynamic factors that influence strategies in determining the most efficient and cost effective methods to mitigate risk of transmission[102]. Additional investigation is still required to improve sensitivity and specificity for preclinical testing that may offer practical application in herd management strategies for trade, relocation, and reintroduction.

1.6 Development of Rat-Adapted Scrapie

Laboratory animals with prion infection offer many advantages in the identification and development of biomarkers. Many factors can be controlled such as known time of infection and ability to track preclinical and clinical disease stages. The most commonly used animals for prion investigation are hamsters and mice. Although infection is well characterized in the hamster model, it is restricted by the lack of genomic and proteomic bioinformatics knowledge, limiting the identification of specific peptides and proteins based upon masses. Furthermore, the volume of CSF obtainable from hamsters is very low (approximately10µl), preventing fractionation schemes that could reduce protein complexity, a critical step for detecting lower abundance proteins[4]. Mice have similar challenges of limited CSF volume available for analysis.

In contrast, the rat provides sufficient CSF to examine disease biomarkers and also has known genomic and proteomic bioinformatics. In a study from Herbst et al, 2015, mouse Rocky Mountain Laboratories (RML) scrapie agent was used for primary passage into female, Sprague-Dawley rats (Figure 1-2)[103]. After one year of incubation, mouse RML scrapie agent was found to transmit into the rat, evidenced by accumulation of PrP^{Sc} in brain homogenate samples after treatment with PK (Figure 1-3). After multiple passages, incubation period stabilized at ~200 days post inoculation (dpi), similar to results from Kimberlin et al[104]. Accumulation of PrP^{Sc} compared to uninfected controls was observed via western blot in 3rd passage and 4th passage and was observed at 117 days post inoculation (dpi) in brain homogenate samples after PK digestion (Figure 1-3). In a subsequent time course study (discussed in the remaining chapters), brain

homogenate samples at an earlier time point of 75 dpi were analysed and PrP^{Sc} accumulation was detected using similar conditions as previously described in Herbst et al, 2015 (Figure 1-4). Histopathological hallmarks, including glial astrocytosis, PrP^{Sc} accumulation and spongiosis, were also observed in the hippocampal region of the diseased brain, (Figure 1-5). CSF samples collected from uninfected and infected rats underwent mass spectrometry analysis. Results identified 10 proteins with an increase in infected rats compared to uninfected, which included known CJD biomarkers, 14-3-3 proteins, and NSE (Table 1-2).

1.7 Hypothesis and Objectives

Many factors have been hypothesized to impact biomarker sensitivity, including disease strain, subtype, duration, age at onset, and timing of lumbar puncture[42, 55, 73, 88, 89, 105-110]. Specificity is determined by comparing detection of prion biomarkers in sCJD to other cohort populations, such as: other prion diseases, other dementias (e.g. Alzheimer's disease), and non-CJD controls[88, 107, 108]. Uniform methods for distinguishing between CJD-infected and uninfected patients using biomarkers are not well defined[111]. For western blot analysis, proteins are scored based on visual assessment of presence or absence of bands where scoring is subject to interpretation, or semi-quantified through densitometry analysis[79, 111]. ELISA offers a quantitative method, however, the cut-off point for determining sensitivity and specificity is determined based on a threshold that is not universal among laboratories[10]. As a result, a wide range of sensitivities and specificities have been reported for CSF biomarkers of CJD[40, 112-114]. For example, 14-3-3 detection was reported to range from 53-97% in sensitivity and 40-100% in specificity depending on the study, demonstrating the variability in test validity[55]. Early testing of prion disease biomarkers was performed on small populations and many cases were not subject to neuropathology confirmation and gave rise to discrepancies[114,115]. Furthermore, the presence of 14-3-3 and NSE in CSF of prion infected patients does not appear to be specific to prion disease; these proteins are present in CSF from patients with other sources of neuronal injury e.g. brain trauma, brain tumors, subarachnoid hemorrhage, stroke, hypoxemia, and encephalitis[116-123] . This lack of specificity may result in false positives if applied to a diverse patient population, therefore, CSF biomarker testing is restricted to patients with strong clinical symptoms indicative of CJD[115, 124, 125]. Because patients are assessed for CSF biomarkers only after clinical onset, the positive predictive values in CJD studies are often overstated[115].

The development of direct methods for testing presence of PrP^{Sc} (RT-QuIC), limits the utility of indirect surrogate markers for diagnostic purposes. However, these markers may still be beneficial for prognosis in terms of predicting stage of prion infection. For example, abundance of 14-3-3 may be related to strain, subtype, and disease duration; presence or absence of this protein has the potential to offer predictions of rate of neuronal death and strain differentiation when assessed over time[45]. Therefore, the objective of this study was to determine if 14-3-3 and NSE offer value in diagnosis and prognosis of prion disease by investigating 1) how known biomarkers would perform in a study where genetic and environmental conditions could be controlled, and 2) if normalization methods (volume vs concentration) would have an effect on biomarker accuracy. We hypothesize that by controlling for these factors, known biomarkers will have greater accuracy in distinguishing between infected and uninfected, and protein abundance will track with prion disease progression (Chapter 2). We also hypothesize that the RAS model will allow for identification of novel biomarkers that may offer greater utility for prognosis in prion disease (Chapter 3).

Table 1-1. Comparison of molecular type, prevalence, age of onset, disease duration, clinical symptoms, and diagnostic findings in sporadic CJD

Molecular Type	Prev. (%)	Onset (years)	Duration (months)	Clinical Symptoms	Diagnostics
MM or MV Type 1 (40%) and 2 (28%)	68	69 (42-89)	4 (1-26)	Rapid dementia Myoclonus 50% ataxia at onset 30% visual impairment	EEG Positive 14-3-3 Positive MRI: Basal ganglia and cortex
VVType 2 (15%) or Type 1 and 2 (3%)	18	65 (45-85)	6 (3-18)	Ataxia at onset Dementia	EEG Negative 14-3-3 Positive MRI: Basal ganglia and thalamus
MV Type 2 (with plaques)	8	65 (48-81)	16 (5-48)	Dementia Ataxia	EEG Negative 14-3-3 Negative in 40% MRI: Basal ganglia and thalamus
MV Type 2 (with plaques and vacuoles)	3	NA	NA	NA	NA
MM or MV Type 2 (with vacuoles)	1	68 (61-75)	20 (12-36)	Dementia Myoclonus Pyramidal signs No ataxia	EEG Negative 14-3-3 Positive MRI: Cortex
MM Type 2 (with thalamo-olivary atrophy)	1	52 (36-71)	16 (8-24)	Insomnia Psychomotor hyperactivity Ataxia Motor signs	EEG Negative 14-3-3 Negative MRI: Thalamus gliosis
VV Type 1	1	39 (24-49)	15 (14-16)	Dementia Myoclonus Pyramidal signs	EEG Negative 14-3-3 Positive MRI: Cortex

Types of sporadic CJD are highly variable based on molecular type (MM, VV, MV – type 1 and 2), prevalence, age at onset, disease duration, and clinical symptoms. Molecular, pathological, and clinical features add complexity to interpretation of diagnostic testing. NA is no published data available. Adapted from Parchi et al, 2011[14], and Sim, 2013[15].

Table 1-2. CSF proteins in RAS infection.

A)

Known Biomarkers
14-3-3 zeta/delta
14-3-3 epsilon
14-3-3 gamma
Neuron-specific Enolase

B)

Novel Biomarkers
Ribonuclease T2
Cathepsin D
Complement Factor H
Granulin
Macrophage Colony Stimulating Factor 1 Receptor
Serine Protease Inhibitor A3N

Mass spectrometry analysis identified ten proteins that were present in prion-infected animals compared to uninfected controls. A) Known markers of prion infection were identified including 14-3-3 and NSE. B) Novel markers of prion infection were also identified including ribonuclease T2.

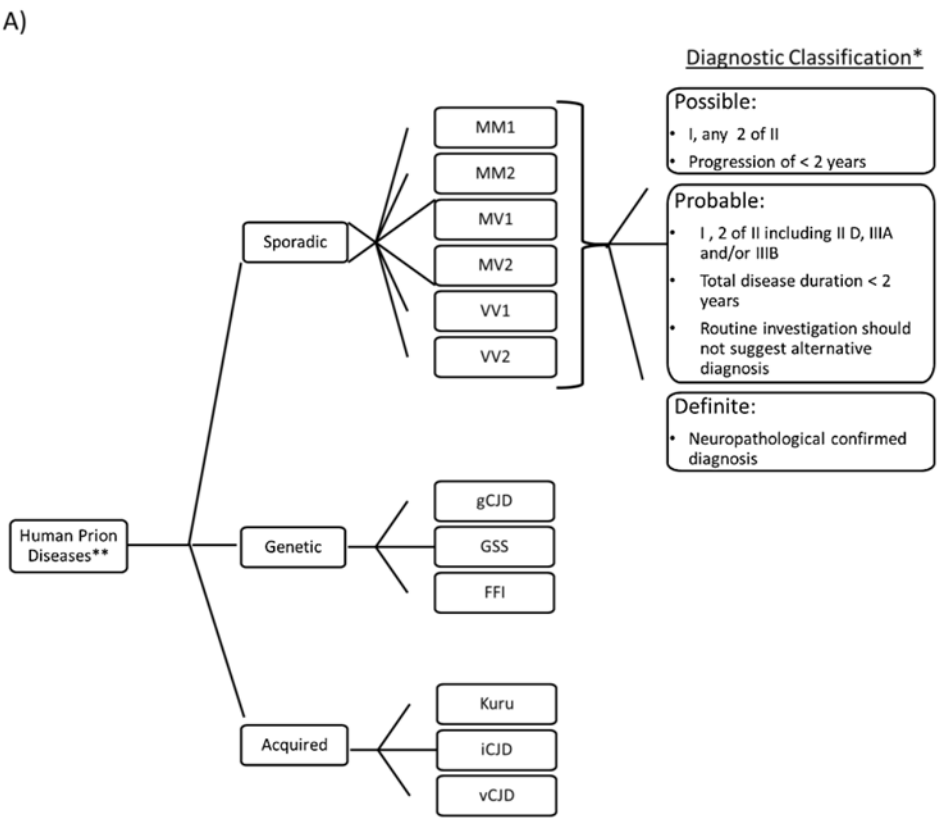

B)

Diagnostic Classification Criteria*		
I		
		Progressive dementia
II		
	A	Myoclonus
	B	Visual or cerebellar problem
	C	Pyrimidal or extrapyrimidal features
	D	Akinetic mutism
III		
	A	Typical EEG
	B	Positive CSF 14-3-3

*Based on WHO diagnostic criteria 1998
**All suspected cases of human prion disease may be subject to EEG, MRI, RT-QuIC, CSF biomarker testing, and genetic screening

Figure 1-1. Schematic for categorization of human prion disease.

A) Human prion diseases can be categorized into sporadic, genetic, and acquired CJD, based on origin. Sporadic CJD types include MM1, MM2, MV1, MV2, VV1, and VV2. Genetic phenotypes include genetic Creutzfeldt-Jakob disease (gCJD), Gerstmann-Straussler-Scheinker disease (GSS), and fatal familial insomnia (FFI). Acquired CJD types include: Kuru, iatrogenic CJD (iCJD), and variant CJD (vCJD). B) Clinical presentation leads to diagnostic testing that may result in possible or probable classification of prion infection. Diagnostic criteria is adapted from World Health Organization diagnostic criteria 1998[16].

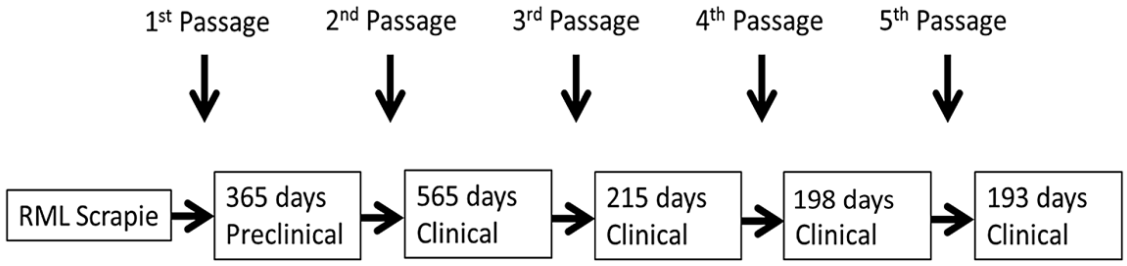

Figure 1-2. Generation of rat-adapted scrapie (RAS).

Rocky Mountain Laboratories (RML) mouse-adapted scrapie was used for transmission to rats. After 1 year of incubation, first passage rats were euthanized to determine the extent of PrP^{Sc} accumulation. PrP^{Sc} was observed and the first passage brain homogenate serially passaged until becoming rat-adapted (indicated by the decrease in and stabilization of the incubation period). Adapted from Herbst et al, 2015[103].

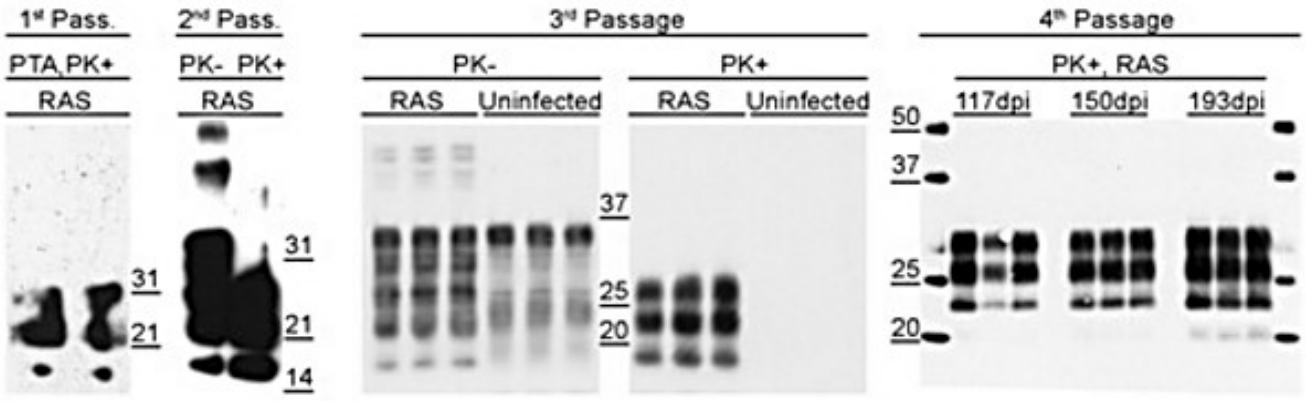

Figure 1-3. Accumulation of PrP^{Sc} in rat-adapted scrapie (RAS).

Brain homogenates from each passage were assayed for the presence of PrP^{Sc} by immunoblot after treatment with Proteinase K (PK). PrP^{Sc} was observed following phosphotungstenic acid (PTA) enrichment at first passage. Di- and mono- glycosylated bands were the most abundant isoforms of PrP^{Sc}. Uninfected age-matched controls are shown for 3rd and 4th passage animals. By fourth passage, PrP^{Sc} accumulated to substantial levels by 117 days post-infection (dpi). Courtesy of Herbst et al, 2015[103].

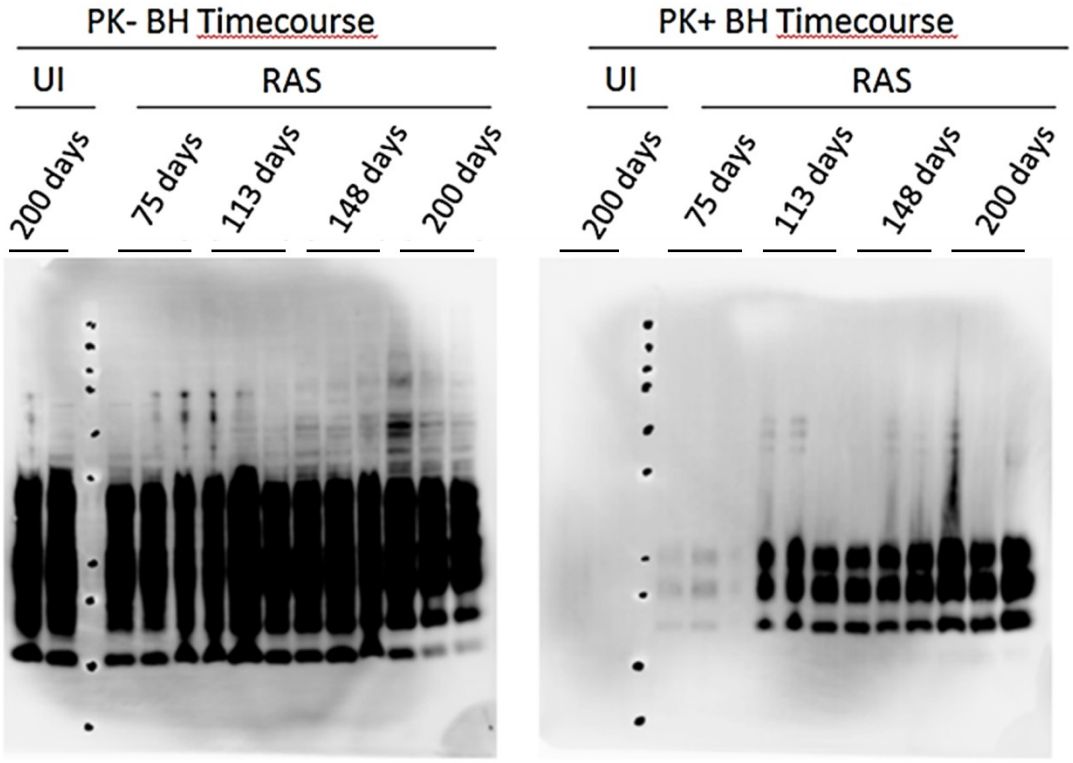

Figure 1-4. Time course detection of PrP^{Sc}

Rat brain homogenate untreated (panel A) and treated with proteinase K (panel B) with n=3 per time point (75, 113, 148, and 200 days post inoculation (dpi)). After PK digestion, PrP^{Sc} remains and is observed as early as 75 dpi.

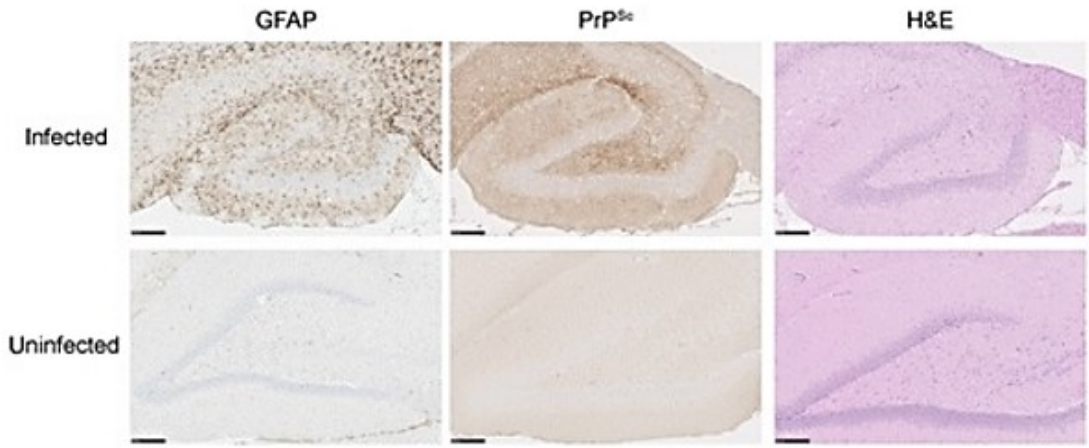

Figure 1-5. Histological analysis of rat-adapted scrapie (RAS) in the hippocampus at clinical disease.

Infected animals showed intense immuno-staining for deposits of PrP^{Sc} and GFAP expressing astrocytes. Spongiform change is an abundant feature in rat prion disease. The scale bar represents 250µm. Courtesy of Herbst et al, 2015[103].

Chapter 2: Lack of Diagnostic and Prognostic Utility of Known Prion Disease Biomarkers

2.1 Introduction

Through use of the rat model, we hypothesized that we would be able to describe the utility of 14-3-3 and NSE for diagnosis and prognosis using a controlled system. Prion infection in the rat i) provides sufficient CSF to examine disease biomarkers that track with disease progression over time, and ii) facilitates analysis of CSF at defined preclinical stages of infection. We hypothesized that by controlling for parameters of prion disease (time of infection, prion strain and dose) and other variables (age, genetic background, and environment), that biomarkers (14-3-3 and NSE) would more accurately differentiate between infected and uninfected animals and track with disease progression.

2.2 Materials and Methods

2.2.1 Ethics Statement

This study was carried out in accordance with the guidelines of the Canadian Council on Animal Care. The protocols used were approved by the Institutional Animal Care and Use Committee at the University of Alberta.

2.2.2 Prion Infection and CSF Collection

Weanling female Sprague Dawley rats were inoculated via intracranial infection with 50µl of 10% rat brain homogenate prepared in water. Signs observed at clinical onset (~180-193 days post inoculation) included porphyrin staining, myoclonus, kyphosis, ataxia, and weight loss. CSF samples from RAS-infected rats were collected at preclinical (75, 113, and 148 (dpi)) and clinical time points (193 dpi), and compared with uninfected, age-matched control samples. Brain tissue was collected from rats infected with rat-adapted scrapie (RAS) at clinical stage and uninfected, age-matched controls as previously described[103]. At specified time points, rats were anesthetized with isoflurane and CSF collected via puncture of the cisterna magna with a 25 gauge neonatal spinal needle (BD Biosciences). CSF volumes of 100-200µL were routinely obtained and scored for blood contamination (Table 2-1). CSF was touch spun for 30s at 2000xg on a benchtop "nano" centrifuge to reduce blood contamination (presence of a red cell pellet) and supernatant was collected. Samples that scored level 3 (+++) or higher for blood contamination were discarded. Samples were frozen and stored at -80˚C.

2.2.3 Immunoblotting

Total protein concentration analysis of CSF samples was performed in duplicate and determined using Pierce BCA protein assay kit. Equal volumes of CSF from each of the 4 samples used in each time point in the pooled data (Figure 2-1) were taken and added to a new 0.5ml microcentrifuge tube and vortexed to make a homologous mixture before adding sample buffer and heated to 100˚C. CSF samples were heated in Laemmli buffer for 10 mins. Bis-Tris SDS-PAGE was performed in duplicates or triplicates (110 volts for 2.5 hours) on 12% polyacrylamide gels (Invitrogen) and transferred on PVDF membrane for western blotting for 2 hours at 35 volts. PVDF membranes were blocked for 1 hour in milk blocking solution (5% milk in Tris buffered saline + Tween 20 (TBS-T)). Two markers for 14-3-3 were chosen for western blot analysis: 14-3-3 pan and 14-3-3 gamma. 14-3-3 pan is recommended by the WHO[16], while 14-3-3 gamma is present in neurons[126]. Antibodies against 14-3-3 pan and 14-3-3 gamma were purchased from Santa Cruz and used a concentration of 1:1000. NSE antibody was purchased from Abcam and used at a dilution of 1:2000. Membranes incubated in primary antibody overnight at 4ºC. Membranes were washed 6 times for 4 minutes in TBS-T before incubating in secondary antibody for 1 hour. The secondary antibody used was goat anti-rabbit HRP used at a concentration of 1:10 000. Membranes were washed and immersed in Pierce ECL western blotting substrate (1:1) for imaging.

2.2.4 Statistical Analysis

Densitometry analysis was performed on western blot data for semi-quantification using Adobe Photoshop CS6 Extended version to determine absolute band intensity. This data was used to generate a receiver operating characteristic (ROC) curve to plot sensitivity vs 1-specificity. The area under the curve (AUC) was calculated to determine the diagnostic accuracy of the biomarkers. ROC curves plot all possible sensitivity/specificity pairs at different thresholds. AUC values were calculated to determine the ability of each marker to accurately distinguish between healthy and prion infected rats [47]. AUC values range between 0.5 and 1, where 0.5 indicates the biomarker is not able to differentiate between infected and uninfected, and 1 indicates 100% sensitivity and specificity and is a perfect result. The AUC is a Mann-Whitney version of the nonparametric two-sample statistic. The ROC curves and AUC values were generated using Graphpad Prism 5 Software.

2.3 Results

2.3.1 Pooled CSF Time Course Characterization

Initial analysis involved pooled samples (equal volumes of CSF from four rats) for each time point and 10ul of sample was loaded per well. Evaluation of pooled samples allowed us to examine the difference in protein levels between infected and uninfected, as well as to refine the timeline for when these differences were observed. Loading by volume was initially chosen as a method of standardization. We observed 14-3-3 and NSE markers early (75 and 113 dpi) in both control and infected animals (Figure 2-1). Presence of these proteins remained in the infected group to clinical time point (193 dpi) but was reduced in control animals over time. Protein biomarker levels in infected groups did not increase or track with disease progression. In addition, 14-3-3 and NSE biomarkers were detected in the control groups at early time points (Figure 2-1), which led us to analyze individual variability.

2.3.2 Individual Variability at 193 Days (Standardized by Volume)

Six samples from clinically infected (193 dpi) and six age-matched controls were standardized by loading 10ul of CSF sample per well (Figure 2-2). Levels of 14-3-3 and NSE detected in western blot analysis showed considerable variability in infected samples. These proteins were also detected in some uninfected controls. The difference between the mean signal of intensity of infected and uninfected was not significant for all markers. AUC values of 0.83 and 0.81 were determined for 14-3-3 pan and gamma respectively with p-values greater than 0.05 (95% confidence interval), indicating that, although there was a trend toward significance, these values were not statistically able to differentiate controls from infected (Table 2-2). NSE had even lower accuracy with an AUC of 0.66 ($p>0.05$), and did not distinguish between infected and uninfected at clinical stage.

2.3.3 Individual Variability at 193 Days (Standardized by Total Protein Concentration)

We subsequently investigated whether variations in protein load could influence detection levels by normalizing total protein concentration (Figure 2-3). Individual samples were standardized by loading 4ug of protein per well. This change in loading resulted in increased AUC values for 14-3-3 and NSE. 14-3-3 pan and gamma displayed an increase in AUC values to 0.99 and 0.97 respectively ($p<0.05$), demonstrating that these tests were accurately able to differentiate

between infected and uninfected, and results were statistically significant. AUC for NSE was found to only marginally increase to 0.75 ($p>0.05$); a significant difference was not found between infected and uninfected individuals for this marker. A summary for comparison of the two methods of standardization is found in Table 2-2.

2.3.4 Individual Variability, Preclinical (Standardized by Volume)

One advantage of the rat prion disease is the ability to study CSF samples at defined preclinical time points. We investigated presence of 14-3-3 and NSE in CSF during preclinical stages of prion infection. Six samples from preclinical time point (148 dpi), and six age-matched controls were standardized by loading 10ul of CSF sample per well and analysed. Analysis of individual animals revealed considerable variability in protein levels for both 14-3-3s and NSE in infected individuals (Figure 2-4). AUC values were 0.58, 0.61, and 0.69 for 14-3-3 pan, gamma, and NSE respectively. Furthermore, levels of these markers were also detected in individual controls. The low AUC values confirmed that these tests were not able to distinguish between diseased and control animals and p-values were not statistically significant ($p>0.05$).

2.4 Discussion

Inconsistencies in reported sensitivities and specificities of 14-3-3 and NSE have brought much debate to the overall utility of these markers for prion disease diagnosis. We hypothesized that standardizing the system would demonstrate consistency and accuracy in biomarker diagnostic testing for prion infection. We utilized the rat, as it allows for the characterization of biomarkers in preclinical and clinical stages in a system that is standardized for numerous confounding factors. In our controlled system, absolute band intensity for 14-3-3 and NSE protein levels were measured from the immunoblot at both preclinical and clinical stages of disease. Biomarker tests were not able to distinguish between animals affected with prion disease and controls when loaded by volume, confirming a lack of diagnostic utility for 14-3-3 and NSE in the rat. New methods for standardizing loading of samples require further investigation. These findings may have implications for use of these markers in current CJD diagnostics.

Studies have investigated CSF biomarkers in “early sCJD” and have tracked biomarker levels over multiple time points[127, 128]. However, these studies have only analyzed biomarkers during early clinical stage of infection and found protein abundance to be highly variable across

individual patients. Using the controlled rat model, we further hypothesized that known prion disease biomarkers such as 14-3-3 and NSE may offer utility in predicting stage of disease for early detection that will aid in prognosis. Results demonstrated that even in this controlled system, 14-3-3 and NSE markers did not track with disease progression and protein levels were highly variable.

Improvements in the ability to detect low levels of PrP^{Sc} in bio-available fluids have been made possible through methods such as RT-QuIC. The effectiveness of RT-QuIC in combination with MRI brings into question the utility of other CSF biomarkers for prion diagnosis. Recently, mouse models have provided evidence that with prion replication and accumulation, there becomes a limitation to substrate availability due to the downregulation of PrP^{C}, causing levels of infectious prion protein in the brain to plateau during the preclinical phase of prion infection[129]. Currently RT-QuIC has only been shown to be effective in clinical onset of prion infection and the "plateau effect" may prevent this method from being useful in prognosis. One objective of this study was to evaluate known prion disease biomarkers to assess prognostic utility in a controlled system. In this study, we found that 14-3-3 and NSE abundance did not increase over the course of infection and remained highly variable in individual RAS samples that were standardized by volume, indicating a lack of prognostic utility for 14-3-3 and NSE for prion infection.

Table 2-1. Blood Contamination Scoring.

Blood contamination Scoring	Definition
-Blood	▪ Colorless, clear supernatant ▪ No visible pellet
Level 1 (+)	▪ Colorless, clear supernatant ▪ Pellet just visible
Level 2 (++)	▪ Colorless, clear supernatant. ▪ Pellet slightly larger
Level 3 (+++)	▪ Xanthochromia (yellowing) ▪ Large pellet
Level 4 (++++)	▪ Red supernatant remaining after touch spin ▪ Large pellet

CSF samples obtained from rats were qualitatively scored for blood contamination based on color of supernatant, and presence of size of red blood cell pellet. Samples that scored level 3 (+++) or higher were discarded.

Table 2-2. A comparison of methods used for standardization.

	Time Point 193 days	
Antibody	**Volume 10µl/well (A)**	**Total Protein Concentration 4µg/µl/well (B)**
14-3-3 Pan	N.S.D between Control and RAS mean AUC=0.83	P value 0.005*** AUC=0.99
14-3-3 Gamma	N.S.D between Control and RAS mean AUC=0.81	P value 0.007*** AUC=0.97
NSE	N.S.D between Control and RAS mean AUC=0.61	N.S.D. between Control and RAS mean AUC=0.75

Loading of individual samples was standardized based on loading by volume (10µl) (A), and by total protein concentration (0.4µg/µl) (B). 14-3-3pan, 14-3-3 gamma, and neuron-specific enolase (NSE) were analysed for both methods of standardization and compared at 193 days post inoculation. Area under the curve (AUC), standard error (Std. Error), 95% confidence interval (CI), and p values are reported. N.S.D. indicates no significant difference. High statistical significance is designated by ***.

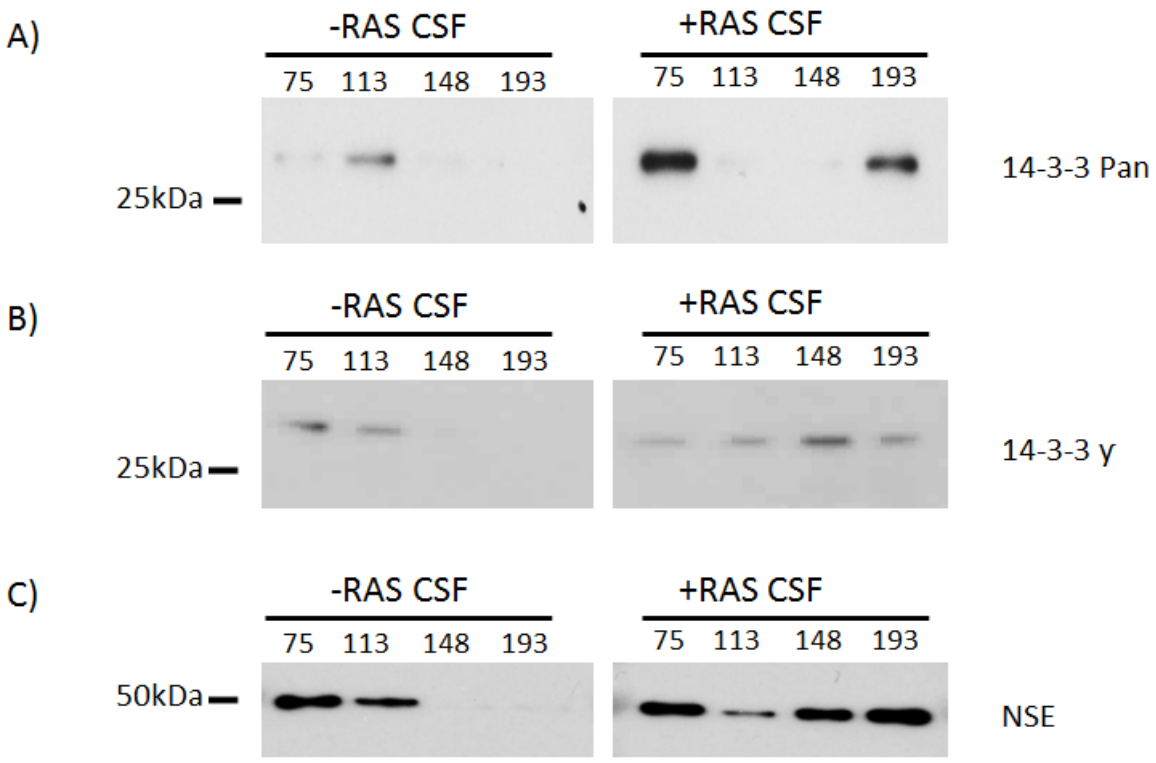

Figure 2-1. Pooled time course characterization of 14-3-3 and NSE in rat-adapted scrapie (RAS) infection

Western blot analysis of pooled CSF (n=4) collected from RAS-infected Sprague-Dawley rats and uninfected age-matched controls over time. CSF from three pre-clinical time points (75dpi, 113dpi, and 148 dpi), as well as a clinical time point (193 dpi), were probed for (Panel A) 14-3-3 pan, (Panel B) 14-3-3 gamma, and (Panel C) NSE.

A)

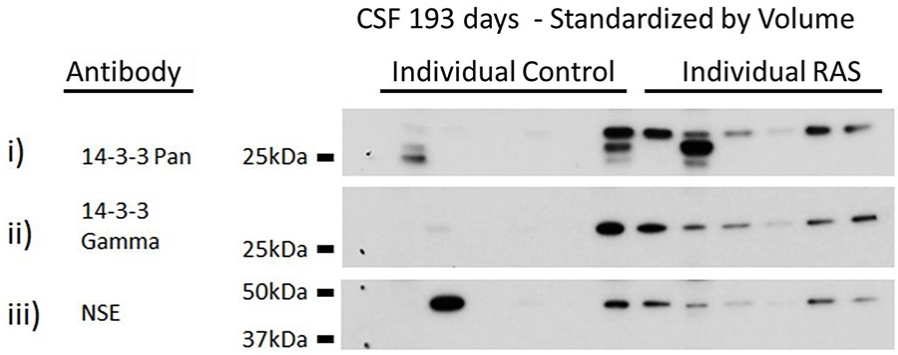

B)

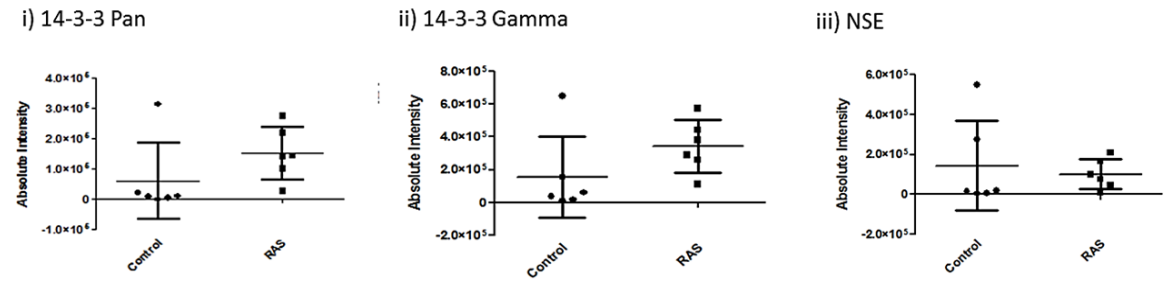

C)

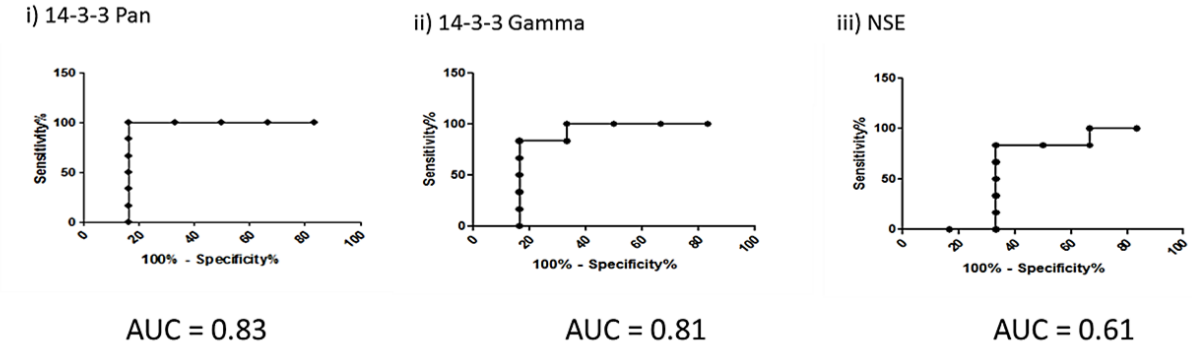

Figure 2-2. Individual characterization of 14-3-3 and NSE in rat-adapted scrapie (RAS) infection standardized by volume.

Western blot analysis of individual CSF samples standardized by volume from RAS infected rats at clinical stage (193 days post inoculation) and age-matched controls. CSF was collected from 6 RAS infected rats at clinical stage and compared to 6 age-matched controls using 14-3-3 pan, 14-3-3 gamma, and NSE antibodies. Panel A) 10µl CSF/well. B) Densitometry analysis of western blot. C) Receiver operating characteristic (ROC) curve with area under the ROC curve (AUC).

A)

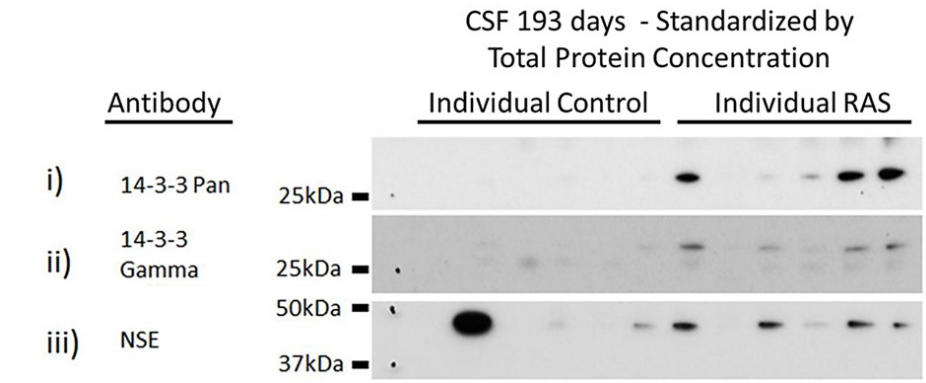

B)

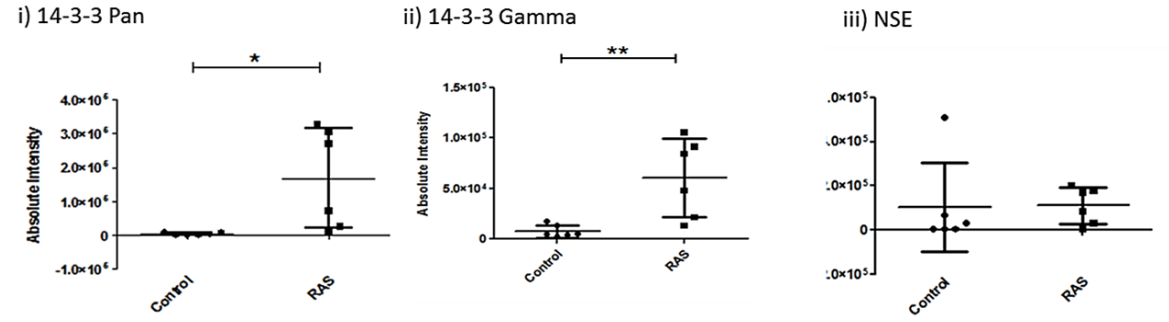

C)

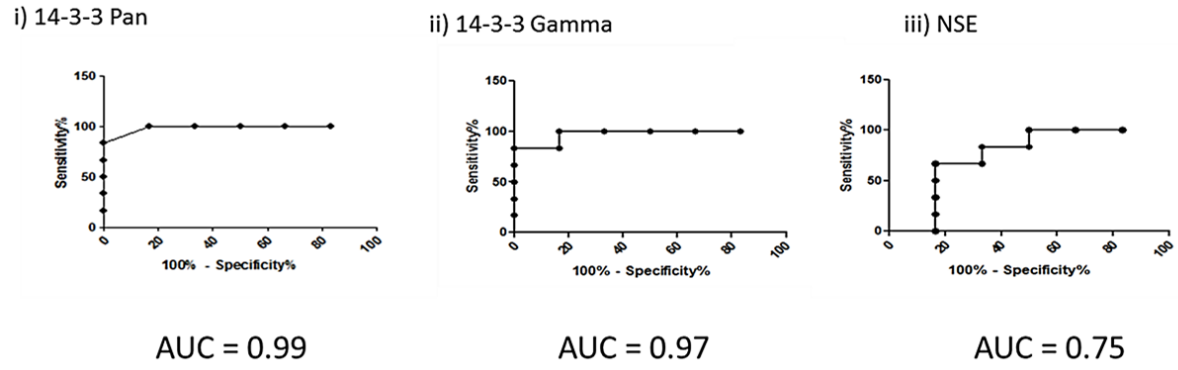

Figure 2-3. Individual characterization of 14-3-3 and NSE in rat-adapted scrapie (RAS) infection standardized by total protein concentration.

Western blot analysis of individual CSF samples standardized by protein concentration from RAS infected rats at clinical stage (193 days post inoculation) and age-matched controls. CSF was collected from 6 RAS infected rats at clinical stage and compared to 6 age-matched controls using 14-3-3 pan, 14-3-3 gamma, and NSE antibodies. Panel A) 4µg total protein loaded/well. B) Densitometry analysis of western blot. C) Receiver operating characteristic (ROC) curve with area under the ROC curve (AUC).

A)

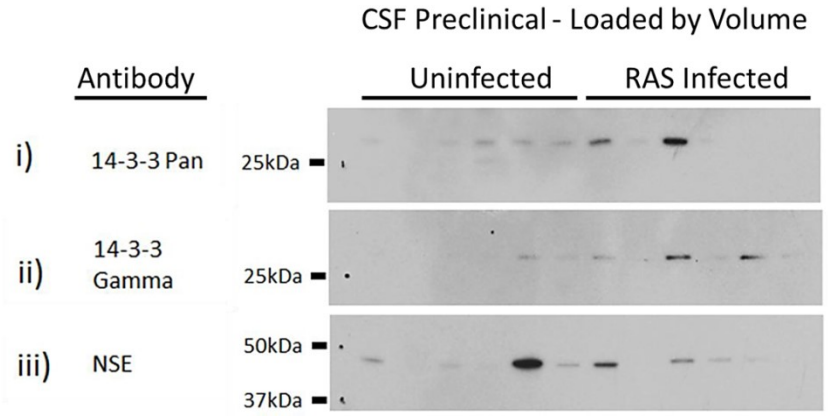

B)

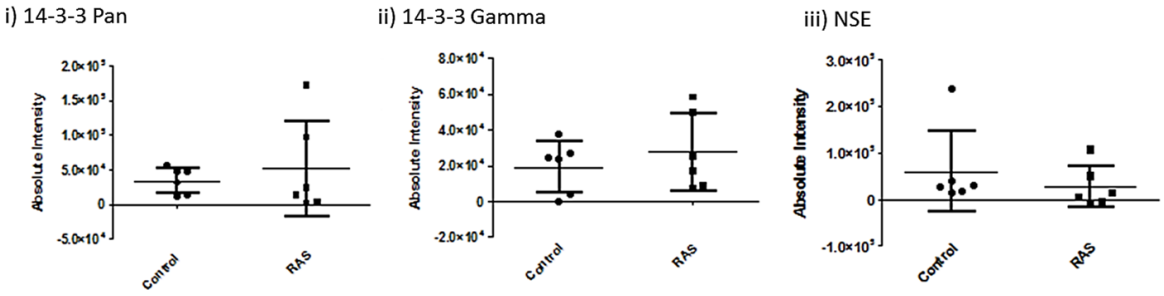

C)

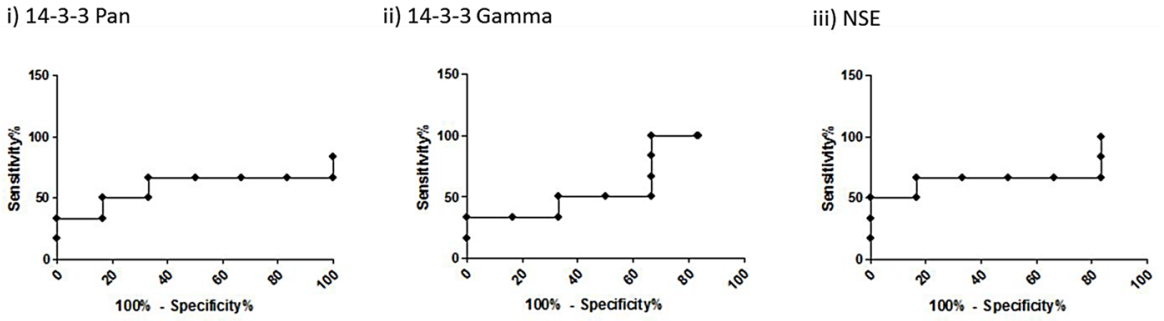

AUC = 0.58 AUC = 0.61 AUC = 0.69

Figure 2-4. Individual characterization of 14-3-3 and NSE in rat-adapted scrapie (RAS) infection, preclinical.

CSF collection from 6 RAS infected rats at preclinical time point (148 days post inoculation) were compared to 6 age-matched controls loaded by total protein. A) Western blot analysis from infected and uninfected individuals of 14-3-3 pan, 14-33- gamma, and NSE. B) Densitometry analysis of western blot. C) Receiver operating characteristic (ROC) curve with area under the ROC curve (AUC).

Chapter 3: Novel Prion Disease Biomarkers

3.1 Introduction

In general, biomarkers are used as a discriminative tool to indicate biological processes such as disease status, pathological process, or response to treatment[130]. These indicators include physical traits, imaging of pathological features, or presence of biological molecules in bodily tissues and fluids. Prion disease biological markers can be divided into 2 categories: pathophysiological markers that reflect prion pathology at any point over the course of infection, and/or topographical markers that may reflect downstream damage[131]. The pathophysiological diagnostic marker of prion infection is PrP^{Sc}; the topographical markers include EEG and MRI, and indirect surrogate markers that may indicate stage of preclinical and clinical status. Currently, biomarker abundance is assessed during clinical onset of prion disease. There is a clear need for early (preclinical) detection of these diseases. A prion disease biomarker that can discriminate prion infection at both preclinical and clinical stages of infection and whose abundance increases with disease progression over time would, in addition to providing early detection, have utility in the assessment therapeutic interventions and have the potential to aid in prognosis.

To define preclinical and clinical stages of prion infection and understand changes in pathobiology over the course of infection, we have established prion infection in the rat. Using this controlled system, known CJD biomarkers, as well as novel biomarkers were identified by analysing CSF from infected compared with uninfected controls using mass spectrometry analysis, as previously described in Chapters 1 and 2. One of the novel biomarkers identified was ribonuclease T2 (RNase T2). This protein is localized in the lysosome and is the only human member of the Rh/T2/S family of acidic hydrolases[132, 133]. The α+β core motif, comprised of 4-8 β sheet with the exterior tertiary structure formed by helices, is highly conserved in bacteria, fungi, and plants despite demonstrating a broad range of functions[134, 135]. The *RNase T2* gene has shown tumor suppressor activity in an ovarian cancer cell line[136], and the plant form of *RNase T2*, Actibind, has also demonstrated tumor suppressor activity[137, 138]. *RNase T2* gene mutations have been associated with white matter disease of the infant human brain and indicate that the protein has a biological role in neurodevelopment[134, 139]. Comparable brain abnormalities have also been described in a transgenic zebra fish model[140]. It has been hypothesized that RNase T2 might play a role in cellular innate immune response processes[133, 141, 142]. Involvement with neurodevelopment and innate immunity, along with the presence of this protein in CSF of prion

infected rats suggests that RNase T2 plays an active role in prion infection. The objective was to characterize the RNase T2 abundance over time of infection and characterize the utility of this candidate biomarker for the diagnosis and prognosis of prion infections.

3.2 Materials and Methods

3.2.1 Ethics Statement

This study was carried out in accordance with the guidelines of the Canadian Council on Animal Care. The protocols used were approved by the Institutional Animal Care and Use Committee at the University of Alberta.

3.2.2 CSF Collection and Immunoblotting

Weanling, female Sprague-Dawley rats were intracranially infected with 50µl of 10% rat brain homogenate and brain tissue and CSF samples were harvested over time and handled as previously described in Chapter 2. Immunoblotting was performed as described by Herbst et al, 2015[103] using standard protocols on 12% Nupage acrylamide gels and PVDF membrane for western blotting. An antibody against RNase T2 was purchased from Abcam and used at a concentration of 1:2000. The secondary antibody used was goat anti-rabbit HRP used at a concentration of 1:10 000.

3.2.3 Statistical Analysis

Densitometry analysis was performed on western blot data for semi-quantification using Adobe Photoshop CS6 Extended version to determine absolute band intensity of the 36 kDa RNase T2. ROC curves and AUC values were generated using Graphpad Prism 5 Software and used to determine the diagnostic accuracy of the biomarkers.

3.3 Results

3.3.1 Pooled CSF Time Course Characterization

Our initial analysis involved using the same pooled samples that were used for 14-3-3 and NSE characterization and normalized by volume in Chapter 2. Although we observed RNase T2 in RAS infected animals and in uninfected age-matched controls (Figure 3-1), an increase in protein abundance was observed in prion infected rats starting at 113 dpi, an increase that continued with

disease progression. In comparison, RNase T2 protein levels remained consistent over time in uninfected controls.

3.3.2 Individual Variability at 193 Days (Standardized by Volume)

Similar to previous examination of known CJD markers, analysis of individual variability was also assessed. Six samples from clinically infected (193 dpi) and six age-matched controls were standardized by loading 10ul of CSF sample per well (Figure 3-2). In contrast to 14-3-3 and NSE, infected samples showed less individual variability and demonstrated increased abundance compared to uninfected controls. The difference between the mean signal of intensity of infected and uninfected was significant ($p<0.0001$). An AUC value of 1.00 was determined for RNase T2, with p-value of 0.004, indicating this biomarker was accurately able to differentiate controls from infected at clinical stage of infection.

3.3.3 Individual Variability at 193 Days (Standardized by Total Protein Concentration)

We investigated normalized total protein concentration to determine if protein load would have an influence on detection levels. Individual samples were standardized by loading 4ug of protein per well (Figure 3-3). This change in loading resulted in a significant difference between the mean signal of intensity of infected and uninfected was significant ($p<0.0001$). an AUC value of 1.00 for RNase T2 demonstrating that protein load did not have a great effect on biomarker accuracy and again demonstrating that this test was able to differentiate between infected and uninfected, and results were statistically significant (p-value = 0.004).

3.3.4 Individual Variability, Preclinical (Standardized by Volume)

We investigated presence of RNase T2 in CSF during preclinical stages of prion infection. Six samples from preclinical time point (148 dpi), and six age-matched controls were standardized by loading 10ul of CSF sample per well and analysed. Analysis of individual animals revealed considerable relatively little individual variability in infected individuals (Figure 3-4). Although RNase T2 was also detected in some uninfected controls, protein abundance was greater in infected individuals. The AUC was 0.94 and found to be statistically significant ($p<0.01$). The AUC value confirmed that RNase T2 biomarker was able to distinguish between diseased and control animals at preclinical time point of 148 days.

3.4 Discussion

We utilized the rat prion infection for novel biomarker identification, as it is a standardized system that can be used to track disease progression over time. Absolute band intensity for RNase T2 levels was measured from the immunoblot for individual samples at clinical stage of disease and compared to age-matched, uninfected controls. This biomarker was able to distinguish between animals affected with prion disease and controls, suggesting a potential diagnostic utility for RNase T2 in the rat. We also observed an increase in abundance of protein levels at preclinical stages, indicating that RNase T2 may offer utility in predicting stage of disease for early detection that will aid in prognosis. There were no significant differences in methods of standardizing loading of protein (volume vs concentration).

Clinical stage of prion infection is defined as the occurrence of clinical phenotype, including prodromal and dementia stages. Preclinical is defined by the presence of biomarker indicators and existence of prion disease pathology in infected animals prior to the exhibition of clinical signs. Further classification is required to better define and characterize stages of preclinical disease. The rat provides a useful model to specify what markers are present/increasing/decreasing in abundance during specific stages of preclinical infection, which can be used to develop and observe effectiveness of therapeutic intervention.

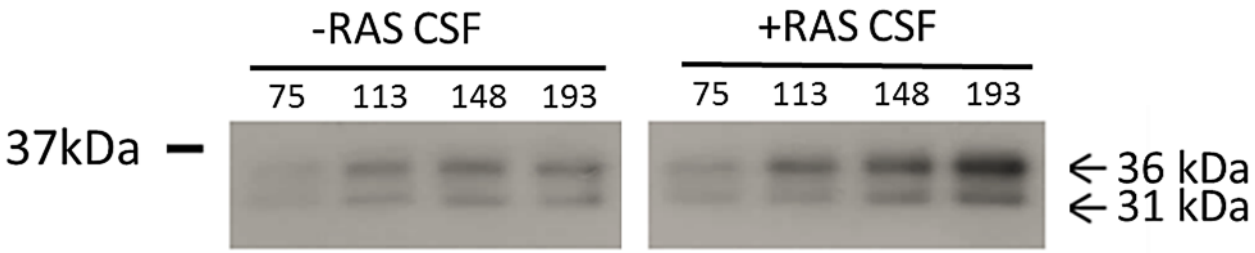

Figure 3-1. RNase T2 Abundance in CSF is elevated in prion infected rats.

Western blot analysis of pooled CSF (n=4) collected from RAS-infected Sprague-Dawley rats and uninfected age-matched controls over time. CSF from three pre-clinical time points (75dpi, 113dpi, and 148 dpi), as well as a clinical time point (193 dpi), were probed for RNase T2. RNase T2 is observed at 36kDa with a shorter isoform at 31 kDa as indicated by arrows. RNase T2 becomes elevated as early as 113 days post infection (Herbst et al, 2016 in preparation).

A)

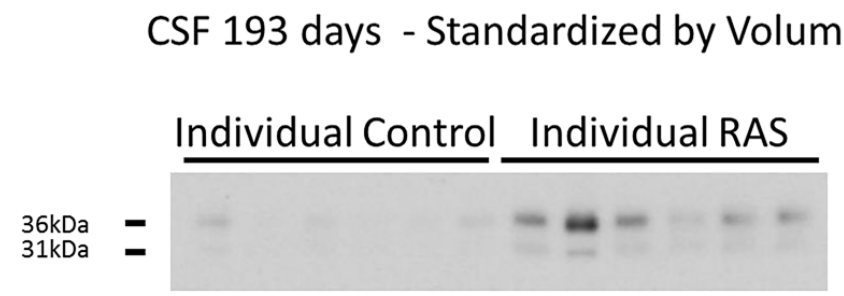

B)

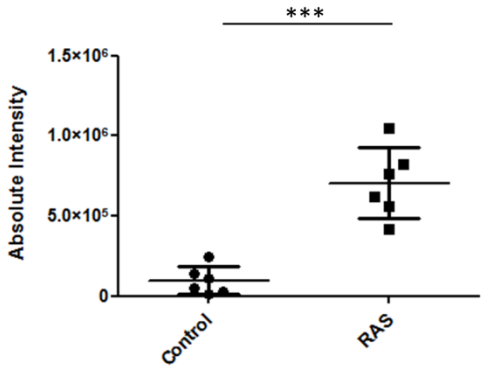

C)

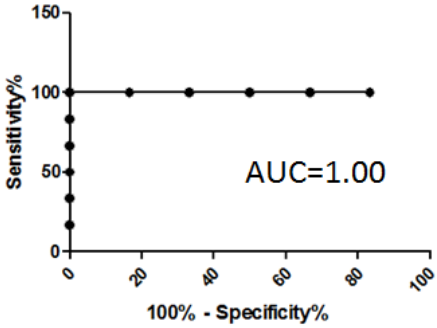

Figure 3-2. **Ribonuclease T2 is elevated at 193 days in rat-adapted scrapie infection Standardized by volume.**

Western blot analysis of individual CSF samples standardized by volume from RAS infected rats at clinical stage (193 days post inoculation) and age-matched controls. CSF was collected from 6 RAS infected rats at clinical stage and compared to 6 age-matched controls using the RNase T2 antibody. Panel A) 10µl CSF/well. B) Densitometry analysis of western blot. C) Receiver operating characteristic (ROC) curve with area under the ROC curve (AUC).

A)

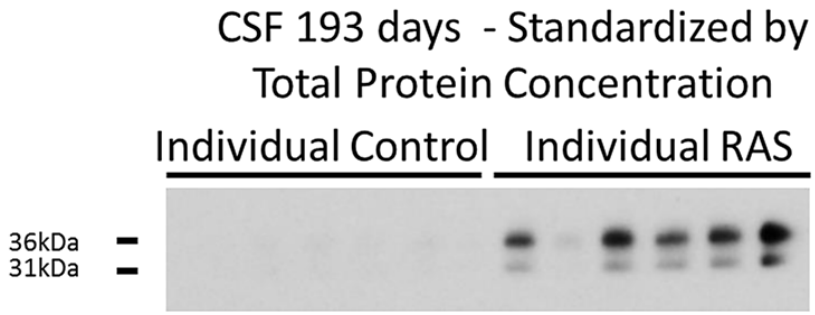

B)

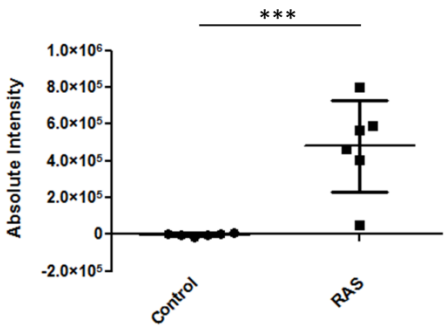

C)

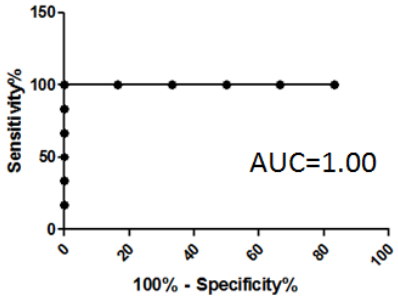

Figure 3-3. **Ribonuclease T2 is elevated at 193 days in rat-adapted scrapie infection Standardized by total protein concentration.**

Western blot analysis of individual CSF samples standardized by protein concentration from RAS infected rats at clinical stage (193 days post inoculation) and age-matched controls. CSF was collected from 6 RAS infected rats at clinical stage and compared to 6 age-matched controls using the RNase T2 antibody. Panel A) 4µg total protein loaded/well. B) Densitometry analysis of western blot. C) Receiver operating characteristic (ROC) curve with area under the ROC curve (AUC).

A)

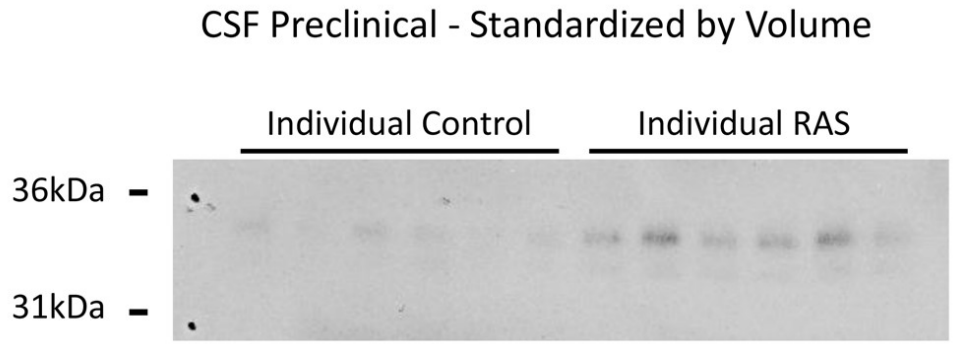

B)

C)

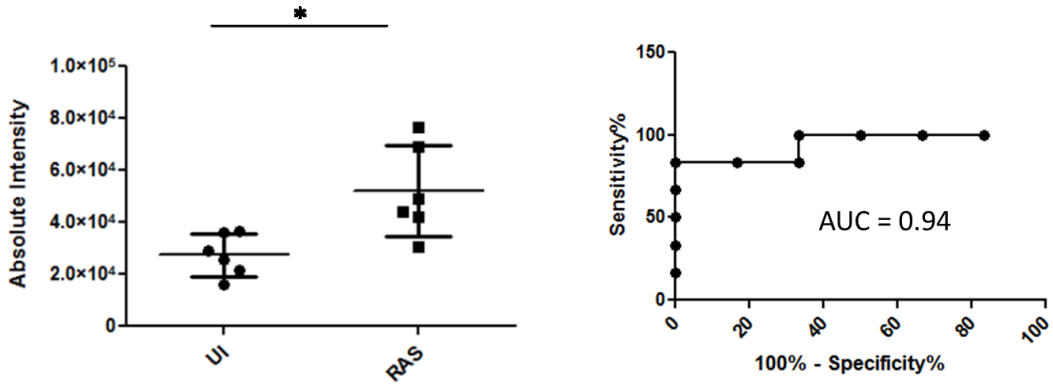

Figure 3-4. **Ribonuclease T2 is elevated in rat-adapted scrapie, preclinical.**

Western blot analysis of individual CSF samples loaded based on volume from RAS infected rats at preclinical stage (148 days post inoculation) and age-matched controls. CSF was collected from 6 RAS infected rats at preclinical stage and compared to 6 age-matched controls using the RNase T2 antibody. Panel A) 10µl CSF/well. B) Densitometry analysis of western blot. C) Receiver operating characteristic (ROC) curve with area under the ROC curve (AUC).

Chapter 4: Conclusions and Future Directions

4.1 Conclusions

The extended preclinical phase and rapid clinical phase of prion disease makes diagnosis and prognosis of prion infection extremely challenging[87]. Definitive diagnosis of human prion diseases, including CJD, involves direct detection of PrP^{Sc} via samples collected post-mortem from the diseased brain[143]. Indirect, ante-mortem methods such as CSF protein biomarkers, EEG, MRI, and RT-QuIC are used in addition to clinical symptoms to assist clinicians in diagnosing suspect CJD cases during the clinical phase of prion disease[38,70]. The rat model provides a system that can be used to investigate and characterize prion disease progression over multiple preclinical and clinical time points and has the potential to be used as a tool for determining efficacy of therapies that are being developed.

The rat remains a useful model that has the potential to aid in novel biomarker identification, as well as for evaluating therapeutic strategies that may be useful for prognosis in human prion diseases. These studies have demonstrated that the rat model can be used for known and novel biomarker identification that can ultimately characterize and uniformly define disease stages from preclinical to full clinical signs over the course of prion disease (Figure 4-1). We were able to determine that there is a lack of utility for known biomarkers' 14-3-3 and NSE for both diagnosis and prognosis in the rat (Table 4-1). Furthermore, we verified that the novel biomarker RNase T2 was able to distinguish between prion-infected rats and age-matched controls and increased in abundance with disease progression, demonstrating potential for use in diagnosis and prognosis of prion infection.

4.2 Future Directions

Variability in testing can occur through all stages of an experiment; differences in pre-analytical protocols, analytical procedures, assay format and quality, and batch-to-batch variation. In humans, variation in testing can also be attributed to factors such as age, genetic susceptibility (M/V) and origin of infection (sporadic, genetic and acquired). These reasons for variation warrant specific cut-offs for biomarkers and universal CSF standardization. There is a need for creating certified reference materials for assay calibration and establishing reference measurement procedures (RMP), as has been done for other fields of neurodegeneration[131]. The controlled rat system can facilitate in determining universal reference measurements.

RNase T2 must be tested in human prion diseases to determine sensitivity and specificity and overall assess applications in human testing. Our mass spectrometry studies of rat CSF also identified additional candidate markers such as complement factor H and cathepsin D that require further validation.

One of the limitations of these studies was not being able to longitudinally track over the course of infection. CSF collection of the same rat over multiple time points may further reduce sample variation. CSF samples were treated uniformly and the risk for blood contamination was taken into consideration by performing relative total protein concentration assays and by creating a scoring system that eliminated samples deemed contaminated. Analysis such as erythrocyte count should be included in future studies to determine quantifiable threshold for levels of contamination that will not have an impact on biomarker results. As new technologies such as the 14-3-3 gamma ELISA assays and advances with electrochemiluminescence become more broadly available, we expect more universal protocols and standardization practices will be developed and more valuable comparisons can be made between detection techniques and across laboratories[126, 144].Testing of current ELISA tests that are available such as the new 14-3-3γ (Circulex 14-3-3 Gamma ELISA Kit, Cyclex Co., Ltd., Nagano, Japan) could be useful to assess the accuracy of this test in a controlled system[145]. Development of ELISA tests for the novel biomarkers identified (RNase T2) on rat CSF samples for quantification of novel protein markers and to develop reference numbers that could be extrapolated and applied to human studies. Employing new technologies such as electrochemiluminescence-based detection systems would allow for less sample to be used and quicker analysis of multiple samples for CSF biomarker quantification[144].

The ultrasensitive RT-QuIC technique has recently been utilized in hospital settings to aid in detection of low levels of PrP^{Sc} in CSF for diagnosing suspected CJD patients, usually after clinical onset of infection. The rat model has the potential to facilitate in the characterization of PrP^{Sc} abundance in CSF samples during the preclinical stage of infection in a controlled system. The rat could be used to determine if PrP^{Sc} abundance increases with disease progression in CSF and can be used as a prognostic tool, or if protein levels reach a plateau, as has been observed in the brain[129]. RT-QuIC, used in combination with other biomarkers that have been validated with this model for prognosis, could facilitate in determining current stage of disease and rate of

disease progression. Disease stages should have universal definitions and be defined based on one or more markers present in CSF, or topographic biomarkers such as EEG and MRI. This system could be applied to creating a characterization system used for standardizing human studies. The limited diagnostic capabilities for detecting atypical types of CJD (genetic and acquired), and the potential for a second wave of vCJD carriers emphasizes the importance of preclinical, antemortem testing of prion diseases.

Table 4-1. Summary of proteins detected in CSF at clinical and preclinical time points and comparison of methods used for standardization.

	Clinical (193 days)		**Preclinical (148 days)**
Antibody	Volume (A)	Total Protein (B)	Volume (A)
14-3-3 Pan	N.S.D AUC=0.83	P value 0.005*** AUC=0.99	N.S.D AUC=0.58
14-3-3 Gamma	N.S.D AUC=0.81	P value 0.007*** AUC=0.97	N.S.D AUC=0.61
NSE	N.S.D AUC=0.61	N.S.D. AUC=0.75	N.S.D AUC=0.69
RNase T2	P value 0.004*** AUC=1.00	P value 0.004*** AUC=1.00	P value 0.01* AUC=0.94

Loading of individual samples was standardized based on loading by volume (10µl) (A), and by total protein concentration (0.4µg/µl) (B). 14-3-3pan, 14-3-3 gamma, neuron-specific enolase (NSE), and ribonuclease T2 (RNase T2) were analysed for both methods of standardization and compared at 193 days post inoculation. Area under the curve (AUC) and p values are reported. N.S.D. indicates no significant difference. High statistical significance is designated by ***.

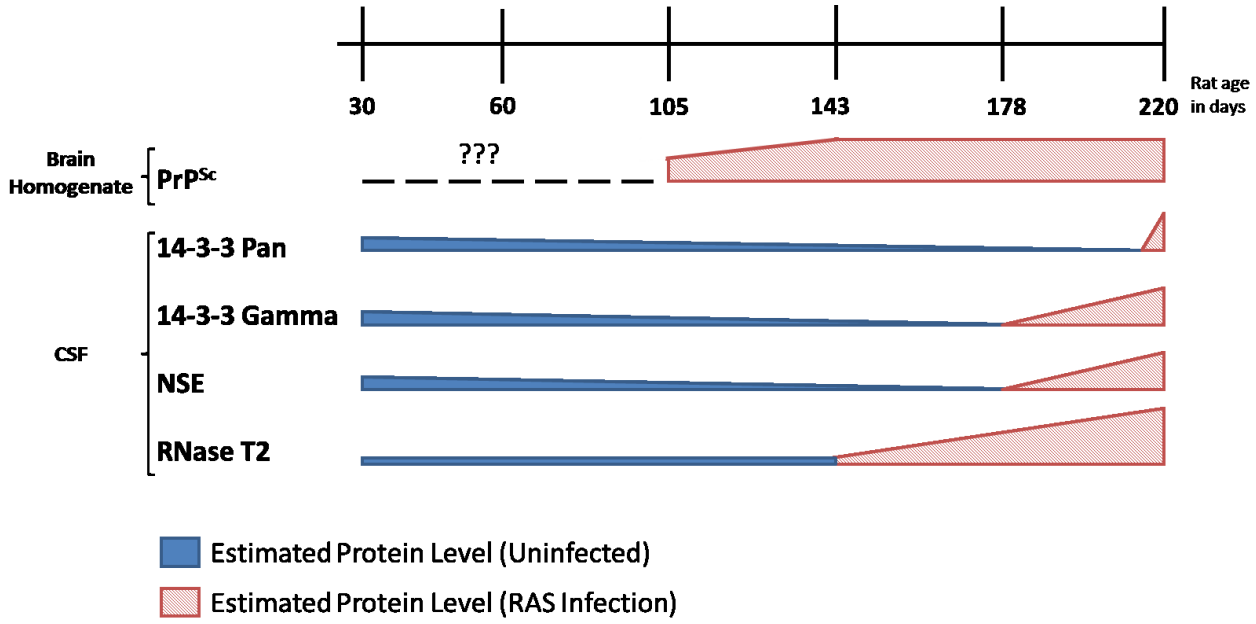

Figure 4-1. Characterization of PrP^{Sc}, 14-3-3 pan, 14-3-3 gamma, and ribonuclease T2 (RNase T2) in rat-adapted scrapie (RAS) infection.

This depiction is based on western blot characterization of proteinase K (PK) digestion of RAS brain homogenate (PrP^{Sc}), and pooled CSF (14-3-3 pan, 14-3-3 gamma, NSE, and RNase T2) from uninfected and infected rats. Blue (solid filled) indicates when biomarkers are present in CSF regardless of infection, and red (pattern filled) indicates when proteins are increasing in abundance due to RAS infection. RNase T2 abundance increases earlier in the course of infection. Note that the abundances between the time points are hypothetical.

References

1. Caughey B, Race RE, Ernst D, Buchmeier MJ, Chesebro B. Prion protein biosynthesis in scrapie-infected and uninfected neuroblastoma cells. J Virol 1989; 63:175-81.

2. Collinge J. Prion diseases of humans and animals: their causes and molecular basis. Annu Rev Neurosci 2001; 24:519-50.

3. Prusiner SB. Prions. Proc Natl Acad Sci U S A 1998; 95:13363-83.

4. Herbst A, McIlwain S, Schmidt JJ, Aiken JM, Page CD, Li L. Prion disease diagnosis by proteomic profiling. J Proteome Res 2009; 8:1030-6.

5. Collinge J, Whitfield J, McKintosh E, Beck J, Mead S, Thomas DJ, Alpers MP. Kuru in the 21st century--an acquired human prion disease with very long incubation periods. Lancet 2006; 367:2068-74.

6. Gough KC, Rees HC, Ives SE, Maddison BC. Methods for Differentiating Prion Types in Food-Producing Animals. Biology (Basel) 2015; 4:785-813.

7. Gambetti P, Kong Q, Zou W, Parchi P, Chen SG. Sporadic and familial CJD: classification and characterisation. Br Med Bull 2003; 66:213-39.

8. Parchi P, Giese A, Capellari S, Brown P, Schulz-Schaeffer W, Windl O, Zerr I, Budka H, Kopp N, Piccardo P, et al. Classification of sporadic Creutzfeldt-Jakob disease based on molecular and phenotypic analysis of 300 subjects. Ann Neurol 1999; 46:224-33.

9. Puoti G, Bizzi A, Forloni G, Safar JG, Tagliavini F, Gambetti P. Sporadic human prion diseases: molecular insights and diagnosis. Lancet Neurol 2012; 11:618-28.

10. Haldiman T, Kim C, Cohen Y, Chen W, Blevins J, Qing L, Cohen ML, Langeveld J, Telling GC, Kong Q, et al. Co-existence of distinct prion types enables conformational evolution of human PrPSc by competitive selection. J Biol Chem 2013; 288:29846-61.

11. Yull HM, Ritchie DL, Langeveld JP, van Zijderveld FG, Bruce ME, Ironside JW, Head MW. Detection of type 1 prion protein in variant Creutzfeldt-Jakob disease. Am J Pathol 2006; 168:151-7.

12. Schoch G, Seeger H, Bogousslavsky J, Tolnay M, Janzer RC, Aguzzi A, Glatzel M. Analysis of prion strains by PrPSc profiling in sporadic Creutzfeldt-Jakob disease. PLoS Med 2006; 3:e14.

13. Cali I, Castellani R, Alshekhlee A, Cohen Y, Blevins J, Yuan J, Langeveld JP, Parchi P, Safar JG, Zou WQ, et al. Co-existence of scrapie prion protein types 1 and 2 in sporadic Creutzfeldt-Jakob disease: its effect on the phenotype and prion-type characteristics. Brain 2009; 132:2643-58.

14. Parchi P, Strammiello R, Giese A, Kretzschmar H. Phenotypic variability of sporadic human prion disease and its molecular basis: past, present, and future. Acta Neuropathol 2011; 121:91-112.

15. Sim VL. Viral Infections of the Human Nervous System: Prion Diseases. 371-392.: Springer Basal, 2013.

16. World Health Organization. Global surveillance, diagnosis and therapy of human transmissible spongioform encephalopathies: report of a WHO consultation. 1998.

17. Chesebro B. Introduction to the transmissible spongiform encephalopathies or prion diseases. Br Med Bull 2003; 66:1-20.

18. Schmitz M, Dittmar K, Llorens F, Gelpi E, Ferrer I, Schulz-Schaeffer WJ, Zerr I. Hereditary Human Prion Diseases: an Update. Mol Neurobiol 2016.

19. Krasnianski A, Heinemann U, Ponto C, Kortt J, Kallenberg K, Varges D, Schulz-Schaeffer WJ, Kretzschmar HA, Zerr I. Clinical findings and diagnosis in genetic prion diseases in Germany. Eur J Epidemiol 2015.

20. Wadsworth JD, Joiner S, Linehan JM, Asante EA, Brandner S, Collinge J. Review. The origin of the prion agent of kuru: molecular and biological strain typing. Philos Trans R Soc Lond B Biol Sci 2008; 363:3747-53.

21. Brown P, Brandel JP, Sato T, Nakamura Y, MacKenzie J, Will RG, Ladogana A, Pocchiari M, Leschek EW, Schonberger LB. Iatrogenic Creutzfeldt-Jakob disease, final assessment. Emerg Infect Dis 2012; 18:901-7.

22. Alpers MP. Review. The epidemiology of kuru: monitoring the epidemic from its peak to its end. Philos Trans R Soc Lond B Biol Sci 2008; 363:3707-13.

23. Gajdusek DC, Gibbs CJ, Alpers M. Experimental transmission of a Kuru-like syndrome to chimpanzees. Nature 1966; 209:794-6.

24. Liberski PP, Sikorska B, Lindenbaum S, Goldfarb LG, McLean C, Hainfellner JA, Brown P. Kuru: genes, cannibals and neuropathology. J Neuropathol Exp Neurol 2012; 71:92-103.

25. Safar JG, Geschwind MD, Deering C, Didorenko S, Sattavat M, Sanchez H, Serban A, Vey M, Baron H, Giles K, et al. Diagnosis of human prion disease. Proc Natl Acad Sci U S A 2005; 102:3501-6.

26. Gibbs CJ, Gajdusek DC, Asher DM, Alpers MP, Beck E, Daniel PM, Matthews WB. Creutzfeldt-Jakob disease (spongiform encephalopathy): transmission to the chimpanzee. Science 1968; 161:388-9.

27. Cervenáková L, Goldfarb LG, Garruto R, Lee HS, Gajdusek DC, Brown P. Phenotype-genotype studies in kuru: implications for new variant Creutzfeldt-Jakob disease. Proc Natl Acad Sci U S A 1998; 95:13239-41.

28. Public Health Agency of Canada. Classic Creutzfeldt-Jakob Disease in Canada Quick Reference Guide. 2007. Accessed March, 2016. www.phac-aspc.gc.ca/nois-sinp/cjd/cjd-eng.php

29. Alberta Health Public Health Notifiable Disease Management Guidelines. Creutzfeldt-Jakob Disease - Classic and Variant, 2013:Pages 1-17. Accessed March, 2016. http://www.health.alberta.ca/documents/Guidelines-Creutzfeldt-Jakob-Disease-2013.pdf

30. Rudge P, Jaunmuktane Z, Adlard P, Bjurstrom N, Caine D, Lowe J, Norsworthy P, Hummerich H, Druyeh R, Wadsworth JD, et al. Iatrogenic CJD due to pituitary-derived growth hormone with genetically determined incubation times of up to 40 years. Brain 2015; 138:3386-99.

31. Llewelyn CA, Hewitt PE, Knight RS, Amar K, Cousens S, Mackenzie J, Will RG. Possible transmission of variant Creutzfeldt-Jakob disease by blood transfusion. Lancet 2004; 363:417-21.

32. National CJD Research Surveillance Unit Data and Reports. Latest NCJDSRU CJD Monthly Statistics. 2016. http://www.cjd.ed.ac.uk/data.html

33. Public Health Agency of Canada. CJD-Surveillance System Statistics. Date accessed: September 13, 2016., 2016. http://www.phac-aspc.gc.ca/hcai-iamss/cjd-mcj/cjdss-ssmcj/stats-eng.php#ref

34. Brown P, Brandel JP, Preece M, Preese M, Sato T. Iatrogenic Creutzfeldt-Jakob disease: the waning of an era. Neurology 2006; 67:389-93.

35. Gill ON, Spencer Y, Richard-Loendt A, Kelly C, Dabaghian R, Boyes L, Linehan J, Simmons M, Webb P, Bellerby P, et al. Prevalent abnormal prion protein in human appendixes after bovine spongiform encephalopathy epizootic: large scale survey. BMJ 2013; 347:f5675.

36. Wroe SJ, Pal S, Siddique D, Hyare H, Macfarlane R, Joiner S, Linehan JM, Brandner S, Wadsworth JD, Hewitt P, et al. Clinical presentation and pre-mortem diagnosis of variant Creutzfeldt-Jakob disease associated with blood transfusion: a case report. Lancet 2006; 368:2061-7.

37. Manix M, Kalakoti P, Henry M, Thakur J, Menger R, Guthikonda B, Nanda A. Creutzfeldt-Jakob disease: updated diagnostic criteria, treatment algorithm, and the utility of brain biopsy. Neurosurg Focus 2015; 39:E2.

38. Zerr I, Pocchiari M, Collins S, Brandel JP, de Pedro Cuesta J, Knight RS, Bernheimer H, Cardone F, Delasnerie-Lauprêtre N, Cuadrado Corrales N, et al. Analysis of EEG and CSF 14-3-3 proteins as aids to the diagnosis of Creutzfeldt-Jakob disease. Neurology 2000; 55:811-5.

39. Young GS, Geschwind MD, Fischbein NJ, Martindale JL, Henry RG, Liu S, Lu Y, Wong S, Liu H, Miller BL, et al. Diffusion-weighted and fluid-attenuated inversion recovery imaging in Creutzfeldt-Jakob disease: high sensitivity and specificity for diagnosis. AJNR Am J Neuroradiol 2005; 26:1551-62.

40. Tschampa HJ, Neumann M, Zerr I, Henkel K, Schröter A, Schulz-Schaeffer WJ, Steinhoff BJ, Kretzschmar HA, Poser S. Patients with Alzheimer's disease and dementia with Lewy bodies mistaken for Creutzfeldt-Jakob disease. J Neurol Neurosurg Psychiatry 2001; 71:33-9.

41. Steinhoff BJ, Zerr I, Glatting M, Schulz-Schaeffer W, Poser S, Kretzschmar HA. Diagnostic value of periodic complexes in Creutzfeldt-Jakob disease. Ann Neurol 2004; 56:702-8.

42. Collins SJ, Sanchez-Juan P, Masters CL, Klug GM, van Duijn C, Poleggi A, Pocchiari M, Almonti S, Cuadrado-Corrales N, de Pedro-Cuesta J, et al. Determinants of diagnostic investigation sensitivities across the clinical spectrum of sporadic Creutzfeldt-Jakob disease. Brain 2006; 129:2278-87.

43. Heath CA, Cooper SA, Murray K, Lowman A, Henry C, MacLeod MA, Stewart G, Zeidler M, McKenzie JM, Knight RS, et al. Diagnosing variant Creutzfeldt-Jakob disease: a retrospective analysis of the first 150 cases in the UK. J Neurol Neurosurg Psychiatry 2011; 82:646-51.

44. Heath CA, Cooper SA, Murray K, Lowman A, Henry C, MacLeod MA, Stewart GE, Zeidler M, MacKenzie JM, Ironside JW, et al. Validation of diagnostic criteria for variant Creutzfeldt-Jakob disease. Ann Neurol 2010; 67:761-70.

45. Parchi P, Saverioni D. Molecular pathology, classification, and diagnosis of sporadic human prion disease variants. Folia Neuropathol 2012; 50:20-45.

46. Mead S. Prion disease genetics. Eur J Hum Genet 2006; 14:273-81.

47. Schröter A, Zerr I, Henkel K, Tschampa HJ, Finkenstaedt M, Poser S. Magnetic resonance imaging in the clinical diagnosis of Creutzfeldt-Jakob disease. Arch Neurol 2000; 57:1751-7.

48. Vitali P, Maccagnano E, Caverzasi E, Henry RG, Haman A, Torres-Chae C, Johnson DY, Miller BL, Geschwind MD. Diffusion-weighted MRI hyperintensity patterns differentiate CJD from other rapid dementias. Neurology 2011; 76:1711-9.

49. Geschwind MD, Potter CA, Sattavat M, Garcia PA, Rosen HJ, Miller BL, DeArmond SJ. Correlating DWI MRI with pathologic and other features of Jakob-Creutzfeldt disease. Alzheimer Dis Assoc Disord 2009; 23:82-7.

50. Zerr I, Kallenberg K, Summers DM, Romero C, Taratuto A, Heinemann U, Breithaupt M, Varges D, Meissner B, Ladogana A, et al. Updated clinical diagnostic criteria for sporadic Creutzfeldt-Jakob disease. Brain 2009; 132:2659-68.

51. Huisman TA. Diffusion-weighted and diffusion tensor imaging of the brain, made easy. Cancer Imaging 2010; 10 Spec no A:S163-71.

52. Naganawa S. The Technical and Clinical Features of 3D-FLAIR in Neuroimaging. Magn Reson Med Sci 2015; 14:93-106.

53. Meissner B, Kallenberg K, Sanchez-Juan P, Collie D, Summers DM, Almonti S, Collins SJ, Smith P, Cras P, Jansen GH, et al. MRI lesion profiles in sporadic Creutzfeldt-Jakob disease. Neurology 2009; 72:1994-2001.

54. Satoh K, Shirabe S, Tsujino A, Eguchi H, Motomura M, Honda H, Tomita I, Satoh A, Tsujihata M, Matsuo H, et al. Total tau protein in cerebrospinal fluid and diffusion-weighted MRI as an early diagnostic marker for Creutzfeldt-Jakob disease. Dement Geriatr Cogn Disord 2007; 24:207-12.

55. Forner SA, Takada LT, Bettcher BM, Lobach IV, Tartaglia MC, Torres-Chae C, Haman A, Thai J, Vitali P, Neuhaus J, et al. Comparing CSF biomarkers and brain MRI in the diagnosis of sporadic Creutzfeldt-Jakob disease. Neurol Clin Pract 2015; 5:116-25.

56. Shiga Y, Miyazawa K, Sato S, Fukushima R, Shibuya S, Sato Y, Konno H, Doh-ura K, Mugikura S, Tamura H, et al. Diffusion-weighted MRI abnormalities as an early diagnostic marker for Creutzfeldt-Jakob disease. Neurology 2004; 63:443-9.

57. Geschwind MD. Rapidly progressive dementia: prion diseases and other rapid dementias. Continuum (Minneap Minn) 2010; 16:31-56.

58. Miele G, Seeger H, Marino D, Eberhard R, Heikenwalder M, Stoeck K, Basagni M, Knight R, Green A, Chianini F, et al. Urinary alpha1-antichymotrypsin: a biomarker of prion infection. PLoS One 2008; 3:e3870.

59. Peden AH, McGuire LI, Appleford NE, Mallinson G, Wilham JM, Orrú CD, Caughey B, Ironside JW, Knight RS, Will RG, et al. Sensitive and specific detection of sporadic Creutzfeldt-Jakob disease brain prion protein using real-time quaking-induced conversion. J Gen Virol 2012; 93:438-49.

60. Orrù CD, Wilham JM, Vascellari S, Hughson AG, Caughey B. New generation QuIC assays for prion seeding activity. Prion 2012; 6:147-52.

61. McGuire LI, Peden AH, Orrú CD, Wilham JM, Appleford NE, Mallinson G, Andrews M, Head MW, Caughey B, Will RG, et al. Real time quaking-induced conversion analysis of cerebrospinal fluid in sporadic Creutzfeldt-Jakob disease. Ann Neurol 2012; 72:278-85.

62. Cosseddu GM, Nonno R, Vaccari G, Bucalossi C, Fernandez-Borges N, Di Bari MA, Castilla J, Agrimi U. Ultra-efficient PrP(Sc) amplification highlights potentialities and pitfalls of PMCA technology. PLoS Pathog 2011; 7:e1002370.

63. Gambetti P, Dong Z, Yuan J, Xiao X, Zheng M, Alshekhlee A, Castellani R, Cohen M, Barria MA, Gonzalez-Romero D, et al. A novel human disease with abnormal prion protein sensitive to protease. Ann Neurol 2008; 63:697-708.

64. Atarashi R, Wilham JM, Christensen L, Hughson AG, Moore RA, Johnson LM, Onwubiko HA, Priola SA, Caughey B. Simplified ultrasensitive prion detection by recombinant PrP conversion with shaking. Nat Methods 2008; 5:211-2.

65. Colby DW, Zhang Q, Wang S, Groth D, Legname G, Riesner D, Prusiner SB. Prion detection by an amyloid seeding assay. Proc Natl Acad Sci U S A 2007; 104:20914-9.

66. Atarashi R, Sano K, Satoh K, Nishida N. Real-time quaking-induced conversion: a highly sensitive assay for prion detection. Prion 2011; 5:150-3.

67. Atarashi R, Satoh K, Sano K, Fuse T, Yamaguchi N, Ishibashi D, Matsubara T, Nakagaki T, Yamanaka H, Shirabe S, et al. Ultrasensitive human prion detection in cerebrospinal fluid by real-time quaking-induced conversion. Nat Med 2011; 17:175-8.

68. Safar J, Wille H, Itri V, Groth D, Serban H, Torchia M, Cohen FE, Prusiner SB. Eight prion strains have PrP(Sc) molecules with different conformations. Nat Med 1998; 4:1157-65.

69. Cramm M, Schmitz M, Karch A, Mitrova E, Kuhn F, Schroeder B, Raeber A, Varges D, Kim YS, Satoh K, et al. Stability and Reproducibility Underscore Utility of RT-QuIC for Diagnosis of Creutzfeldt-Jakob Disease. Mol Neurobiol 2015.

70. Coulthart MB, Jansen GH, Olsen E, Godal DL, Connolly T, Choi BC, Wang Z, Cashman NR. Diagnostic accuracy of cerebrospinal fluid protein markers for sporadic Creutzfeldt-Jakob disease in Canada: a 6-year prospective study. BMC Neurol 2011; 11:133.

71. Park JH, Choi YG, Lee YJ, Park SJ, Choi HS, Choi KC, Choi EK, Kim YS. Real-Time Quaking-Induced Conversion Analysis for the Diagnosis of Sporadic Creutzfeldt-Jakob Disease in Korea. J Clin Neurol 2015.

72. Hsich G, Kenney K, Gibbs CJ, Lee KH, Harrington MG. The 14-3-3 brain protein in cerebrospinal fluid as a marker for transmissible spongiform encephalopathies. N Engl J Med 1996; 335:924-30.

73. Sanchez-Juan P, Sánchez-Valle R, Green A, Ladogana A, Cuadrado-Corrales N, Mitrová E, Stoeck K, Sklaviadis T, Kulczycki J, Hess K, et al. Influence of timing on CSF tests value for Creutzfeldt-Jakob disease diagnosis. J Neurol 2007; 254:901-6.

74. Aitken A, Amess B, Howell S, Jones D, Martin H, Patel Y, Robinson K, Toker A. The role of specific isoforms of 14-3-3 protein in regulating protein kinase activity in the brain. Biochem Soc Trans 1992; 20:607-11.

75. Aitken A, Collinge DB, van Heusden BP, Isobe T, Roseboom PH, Rosenfeld G, Soll J. 14-3-3 proteins: a highly conserved, widespread family of eukaryotic proteins. Trends Biochem Sci 1992; 17:498-501.

76. Boston PF, Jackson P, Thompson RJ. Human 14-3-3 protein: radioimmunoassay, tissue distribution, and cerebrospinal fluid levels in patients with neurological disorders. J Neurochem 1982; 38:1475-82.

77. Sánchez-Valle R, Saiz A, Graus F. 14-3-3 Protein isoforms and atypical patterns of the 14-3-3 assay in the diagnosis of Creutzfeldt-Jakob disease. Neurosci Lett 2002; 320:69-72.

78. Fu H, Subramanian RR, Masters SC. 14-3-3 proteins: structure, function, and regulation. Annu Rev Pharmacol Toxicol 2000; 40:617-47.

79. Schmitz M, Ebert E, Stoeck K, Karch A, Collins S, Calero M, Sklaviadis T, Laplanche JL, Golanska E, Baldeiras I, et al. Validation of 14-3-3 Protein as a Marker in Sporadic Creutzfeldt-Jakob Disease Diagnostic. Mol Neurobiol 2015.

80. Poser S, Mollenhauer B, Kraubeta A, Zerr I, Steinhoff BJ, Schroeter A, Finkenstaedt M, Schulz-Schaeffer WJ, Kretzschmar HA, Felgenhauer K. How to improve the clinical diagnosis of Creutzfeldt-Jakob disease. Brain 1999; 122 (Pt 12):2345-51.

81. Zerr I, Bodemer M, Otto M, Poser S, Windl O, Kretzschmar HA, Gefeller O, Weber T. Diagnosis of Creutzfeldt-Jakob disease by two-dimensional gel electrophoresis of cerebrospinal fluid. Lancet 1996; 348:846-9.

82. Hajduková L, Sobek O, Prchalová D, Bílková Z, Koudelková M, Lukášková J, Matuchová I. Biomarkers of Brain Damage: S100B and NSE Concentrations in Cerebrospinal Fluid--A Normative Study. Biomed Res Int 2015; 2015:379071.

83. Vizin T, Kos J. Gamma-enolase: a well-known tumour marker, with a less-known role in cancer. Radiol Oncol 2015; 49:217-26.

84. Hårdemark HG, Persson L, Bolander HG, Hillered L, Olsson Y, Påhlman S. Neuron-specific enolase is a marker of cerebral ischemia and infarct size in rat cerebrospinal fluid. Stroke 1988; 19:1140-4.

85. Zerr I, Bodemer M, Räcker S, Grosche S, Poser S, Kretzschmar HA, Weber T. Cerebrospinal fluid concentration of neuron-specific enolase in diagnosis of Creutzfeldt-Jakob disease. Lancet 1995; 345:1609-10.

86. Aksamit AJ, Preissner CM, Homburger HA. Quantitation of 14-3-3 and neuron-specific enolase proteins in CSF in Creutzfeldt-Jakob disease. Neurology 2001; 57:728-30.

87. Muayqil T, Gronseth G, Camicioli R. Evidence-based guideline: diagnostic accuracy of CSF 14-3-3 protein in sporadic Creutzfeldt-Jakob disease: report of the guideline development subcommittee of the American Academy of Neurology. Neurology 2012; 79:1499-506.

88. Sanchez-Juan P, Green A, Ladogana A, Cuadrado-Corrales N, Sáanchez-Valle R, Mitrováa E, Stoeck K, Sklaviadis T, Kulczycki J, Hess K, et al. CSF tests in the differential diagnosis of Creutzfeldt-Jakob disease. Neurology 2006; 67:637-43.

89. Green AJ, Thompson EJ, Stewart GE, Zeidler M, McKenzie JM, MacLeod MA, Ironside JW, Will RG, Knight RS. Use of 14-3-3 and other brain-specific proteins in CSF in the diagnosis of variant Creutzfeldt-Jakob disease. J Neurol Neurosurg Psychiatry 2001; 70:744-8.

90. Otto M, Stein H, Szudra A, Zerr I, Bodemer M, Gefeller O, Poser S, Kretzschmar HA, Mäder M, Weber T. S-100 protein concentration in the cerebrospinal fluid of patients with Creutzfeldt-Jakob disease. J Neurol 1997; 244:566-70.

91. Donato R, Cannon BR, Sorci G, Riuzzi F, Hsu K, Weber DJ, Geczy CL. Functions of S100 proteins. Curr Mol Med 2013; 13:24-57.

92. Mietelska-Porowska A, Wasik U, Goras M, Filipek A, Niewiadomska G. Tau protein modifications and interactions: their role in function and dysfunction. Int J Mol Sci 2014; 15:4671-713.

93. Otto M, Wiltfang J, Tumani H, Zerr I, Lantsch M, Kornhuber J, Weber T, Kretzschmar HA, Poser S. Elevated levels of tau-protein in cerebrospinal fluid of patients with Creutzfeldt-Jakob disease. Neurosci Lett 1997; 225:210-2.

94. Boden LA, Houston F, Fryer HR, Kao RR. Use of a preclinical test in the control of classical scrapie. J Gen Virol 2010; 91:2642-50.

95. Haley NJ, Siepker C, Walter WD, Thomsen BV, Greenlee JJ, Lehmkuhl AD, Richt JA. Antemortem Detection of Chronic Wasting Disease Prions in Nasal Brush Collections and Rectal Biopsy Specimens from White-Tailed Deer by Real-Time Quaking-Induced Conversion. J Clin Microbiol 2016; 54:1108-16.

96. Department of Environment, Food, and Rural Affairs and Animal and Plant Health Agency. Cervid spongiform encephalopathy in Norway. June 3, 2016. https://www.gov.uk/government/publications/cervid-spongiform-encephalopathy-in-norway

97. Naylor M. Several moose have caught fatal disease. June 5, 2016. http://norwaytoday.info/news/several-moose-caught-fatal-disease/

98. Haley NJ, Siepker C, Hoon-Hanks LL, Mitchell G, Walter WD, Manca M, Monello RJ, Powers JG, Wild MA, Hoover EA, et al. Seeded Amplification of Chronic Wasting Disease Prions in Nasal Brushings and Recto-anal Mucosa-Associated Lymphoid Tissues from Elk by Real-Time Quaking-Induced Conversion. J Clin Microbiol 2016; 54:1117-26.

99. Spraker TR, VerCauteren KC, Gidlewski T, Schneider DA, Munger R, Balachandran A, O'Rourke KI. Antemortem detection of PrPCWD in preclinical, ranch-raised Rocky Mountain elk (Cervus elaphus nelsoni) by biopsy of the rectal mucosa. J Vet Diagn Invest 2009; 21:15-24.

100. van Keulen LJ, Schreuder BE, Meloen RH, Mooij-Harkes G, Vromans ME, Langeveld JP. Immunohistochemical detection of prion protein in lymphoid tissues of sheep with natural scrapie. J Clin Microbiol 1996; 34:1228-31.

101. Wilham JM, Orrú CD, Bessen RA, Atarashi R, Sano K, Race B, Meade-White KD, Taubner LM, Timmes A, Caughey B. Rapid end-point quantitation of prion seeding activity with sensitivity comparable to bioassays. PLoS Pathog 2010; 6:e1001217.

102. Boden L, Handel I, Hawkins N, Houston F, Fryer H, Kao R. An economic evaluation of preclinical testing strategies compared to the compulsory scrapie flock scheme in the control of classical scrapie. PLoS One 2012; 7:e32884.

103. Herbst A, Ness A, Johnson CJ, McKenzie D, Aiken JM. Transcriptomic responses to prion disease in rats. BMC Genomics 2015; 16:682.

104. Kimberlin RH, Cole S, Walker CA. Temporary and permanent modifications to a single strain of mouse scrapie on transmission to rats and hamsters. J Gen Virol 1987; 68 (Pt 7):1875-81.

105. Baldeiras IE, Ribeiro MH, Pacheco P, Machado A, Santana I, Cunha L, Oliveira CR. Diagnostic value of CSF protein profile in a Portuguese population of sCJD patients. J Neurol 2009; 256:1540-50.

106. Cramm M, Schmitz M, Karch A, Zafar S, Varges D, Mitrova E, Schroeder B, Raeber A, Kuhn F, Zerr I. Characteristic CSF prion seeding efficiency in humans with prion diseases. Mol Neurobiol 2015; 51:396-405.

107. Ladogana A, Sanchez-Juan P, Mitrová E, Green A, Cuadrado-Corrales N, Sánchez-Valle R, Koscova S, Aguzzi A, Sklaviadis T, Kulczycki J, et al. Cerebrospinal fluid biomarkers in human genetic transmissible spongiform encephalopathies. J Neurol 2009; 256:1620-8.

108. Gmitterová K, Heinemann U, Bodemer M, Krasnianski A, Meissner B, Kretzschmar HA, Zerr I. 14-3-3 CSF levels in sporadic Creutzfeldt-Jakob disease differ across molecular subtypes. Neurobiol Aging 2009; 30:1842-50.

109. Sanchez-Valle R, Graus F, Saiz A. Discrepancies in the clinical utility of the 14-3-3 protein for the diagnosis of sporadic Creutzfeldt-Jakob disease. Arch Neurol 2004; 61:604.

110. Castellani RJ, Colucci M, Xie Z, Zou W, Li C, Parchi P, Capellari S, Pastore M, Rahbar MH, Chen SG, et al. Sensitivity of 14-3-3 protein test varies in subtypes of sporadic Creutzfeldt-Jakob disease. Neurology 2004; 63:436-42.

111. Satoh K, Tobiume M, Matsui Y, Mutsukura K, Nishida N, Shiga Y, Eguhchi K, Shirabe S, Sata T. Establishment of a standard 14-3-3 protein assay of cerebrospinal fluid as a diagnostic tool for Creutzfeldt-Jakob disease. Lab Invest 2010; 90:1637-44.

112. Geschwind MD, Martindale J, Miller D, DeArmond SJ, Uyehara-Lock J, Gaskin D, Kramer JH, Barbaro NM, Miller BL. Challenging the clinical utility of the 14-3-3 protein for the diagnosis of sporadic Creutzfeldt-Jakob disease. Arch Neurol 2003; 60:813-6.

113. Perry DC, Geschwind MD. Thorough work-up and new diagnostic criteria needed for CJD. Nat Rev Neurol 2011; 7:479-80.

114. Chitravas N, Jung RS, Kofskey DM, Blevins JE, Gambetti P, Leigh RJ, Cohen ML. Treatable neurological disorders misdiagnosed as Creutzfeldt-Jakob disease. Ann Neurol 2011; 70:437-44.

115. Hamlin C, Puoti G, Berri S, Sting E, Harris C, Cohen M, Spear C, Bizzi A, Debanne SM, Rowland DY. A comparison of tau and 14-3-3 protein in the diagnosis of Creutzfeldt-Jakob disease. Neurology 2012; 79:547-52.

116. Shimada T, Fournier AE, Yamagata K. Neuroprotective function of 14-3-3 proteins in neurodegeneration. Biomed Res Int 2013; 2013:564534.

117. Shiga Y, Wakabayashi H, Miyazawa K, Kido H, Itoyama Y. 14-3-3 protein levels and isoform patterns in the cerebrospinal fluid of Creutzfeldt-Jakob disease patients in the progressive and terminal stages. J Clin Neurosci 2006; 13:661-5.

118. Boesenberg-Grosse C, Schulz-Schaeffer WJ, Bodemer M, Ciesielczyk B, Meissner B, Krasnianski A, Bartl M, Heinemann U, Varges D, Eigenbrod S, et al. Brain-derived proteins in the CSF: do they correlate with brain pathology in CJD? BMC Neurol 2006; 6:35.

119. Stoeck K, Sanchez-Juan P, Gawinecka J, Green A, Ladogana A, Pocchiari M, Sanchez-Valle R, Mitrova E, Sklaviadis T, Kulczycki J, et al. Cerebrospinal fluid biomarker supported diagnosis of Creutzfeldt-Jakob disease and rapid dementias: a longitudinal multicentre study over 10 years. Brain 2012; 135:3051-61.

120. Jacobi C, Reiber H. Clinical relevance of increased neuron-specific enolase concentration in cerebrospinal fluid. Clin Chim Acta 1988; 177:49-54.

121. Vermuyten K, Lowenthal A, Karcher D. Detection of neuron specific enolase concentrations in cerebrospinal fluid from patients with neurological disorders by means of a sensitive enzyme immunoassay. Clin Chim Acta 1990; 187:69-78.

122. Kropp S, Zerr I, Schulz-Schaeffer WJ, Riedemann C, Bodemer M, Laske C, Kretzschmar HA, Poser S. Increase of neuron-specific enolase in patients with Creutzfeldt-Jakob disease. Neurosci Lett 1999; 261:124-6.

123. Steinacker P, Schwarz P, Reim K, Brechlin P, Jahn O, Kratzin H, Aitken A, Wiltfang J, Aguzzi A, Bahn E, et al. Unchanged survival rates of 14-3-3gamma knockout mice after inoculation with pathological prion protein. Mol Cell Biol 2005; 25:1339-46.

124. Burkhard PR, Sanchez JC, Landis T, Hochstrasser DF. CSF detection of the 14-3-3 protein in unselected patients with dementia. Neurology 2001; 56:1528-33.

125. Zerr I, Bodemer M, Gefeller O, Otto M, Poser S, Wiltfang J, Windl O, Kretzschmar HA, Weber T. Detection of 14-3-3 protein in the cerebrospinal fluid supports the diagnosis of Creutzfeldt-Jakob disease. Ann Neurol 1998; 43:32-40.

126. Matsui Y, Satoh K, Miyazaki T, Shirabe S, Atarashi R, Mutsukura K, Satoh A, Kataoka Y, Nishida N. High sensitivity of an ELISA kit for detection of the gamma-isoform of 14-3-3 proteins: usefulness in laboratory diagnosis of human prion disease. BMC Neurol 2011; 11:120.

127. Pennington C, Chohan G, Mackenzie J, Andrews M, Will R, Knight R, Green A. The role of cerebrospinal fluid proteins as early diagnostic markers for sporadic Creutzfeldt-Jakob disease. Neurosci Lett 2009; 455:56-9.

128. Torres M, Cartier L, Matamala JM, Hernández N, Woehlbier U, Hetz C. Altered Prion protein expression pattern in CSF as a biomarker for Creutzfeldt-Jakob disease. PLoS One 2012; 7:e36159.

129. Mays CE, van der Merwe J, Kim C, Haldiman T, McKenzie D, Safar JG, Westaway D. Prion Infectivity Plateaus and Conversion to Symptomatic Disease Originate from Falling Precursor Levels and Increased Levels of Oligomeric PrPSc Species. J Virol 2015; 89:12418-26.

130. Huzarewich RL, Siemens CG, Booth SA. Application of "omics" to prion biomarker discovery. J Biomed Biotechnol 2010; 2010:613504.

131. Dubois B, Hampel H, Feldman HH, Scheltens P, Aisen P, Andrieu S, Bakardjian H, Benali H, Bertram L, Blennow K, et al. Preclinical Alzheimer's disease: Definition, natural history, and diagnostic criteria. Alzheimers Dement 2016; 12:292-323.

132. Campomenosi P, Salis S, Lindqvist C, Mariani D, Nordström T, Acquati F, Taramelli R. Characterization of RNASET2, the first human member of the Rh/T2/S family of glycoproteins. Arch Biochem Biophys 2006; 449:17-26.

133. Thorn A, Steinfeld R, Ziegenbein M, Grapp M, Hsiao HH, Urlaub H, Sheldrick GM, Gärtner J, Krätzner R. Structure and activity of the only human RNase T2. Nucleic Acids Res 2012; 40:8733-42.

134. Luhtala N, Parker R. T2 Family ribonucleases: ancient enzymes with diverse roles. Trends Biochem Sci 2010; 35:253-9.

135. Vidalino L, Monti L, Haase A, Moro A, Acquati F, Taramelli R, Macchi P. Intracellular trafficking of RNASET2, a novel component of P-bodies. Biol Cell 2012; 104:13-21.

136. Acquati F, Possati L, Ferrante L, Campomenosi P, Talevi S, Bardelli S, Margiotta C, Russo A, Bortoletto E, Rocchetti R, et al. Tumor and metastasis suppression by the human RNASET2 gene. Int J Oncol 2005; 26:1159-68.

137. Schwartz B, Shoseyov O, Melnikova VO, McCarty M, Leslie M, Roiz L, Smirnoff P, Hu GF, Lev D, Bar-Eli M. ACTIBIND, a T2 RNase, competes with angiogenin and inhibits human melanoma growth, angiogenesis, and metastasis. Cancer Res 2007; 67:5258-66.

138. Roiz L, Smirnoff P, Bar-Eli M, Schwartz B, Shoseyov O. ACTIBIND, an actin-binding fungal T2-RNase with antiangiogenic and anticarcinogenic characteristics. Cancer 2006; 106:2295-308.

139. Henneke M, Diekmann S, Ohlenbusch A, Kaiser J, Engelbrecht V, Kohlschütter A, Krätzner R, Madruga-Garrido M, Mayer M, Opitz L, et al. RNASET2-deficient cystic leukoencephalopathy resembles congenital cytomegalovirus brain infection. Nat Genet 2009; 41:773-5.

140. Haud N, Kara F, Diekmann S, Henneke M, Willer JR, Hillwig MS, Gregg RG, Macintosh GC, Gärtner J, Alia A, et al. rnaset2 mutant zebrafish model familial cystic leukoencephalopathy and reveal a role for RNase T2 in degrading ribosomal RNA. Proc Natl Acad Sci U S A 2011; 108:1099-103.

141. Everts B, Perona-Wright G, Smits HH, Hokke CH, van der Ham AJ, Fitzsimmons CM, Doenhoff MJ, van der Bosch J, Mohrs K, Haas H, et al. Omega-1, a glycoprotein secreted by Schistosoma mansoni eggs, drives Th2 responses. J Exp Med 2009; 206:1673-80.

142. Steinfelder S, Andersen JF, Cannons JL, Feng CG, Joshi M, Dwyer D, Caspar P, Schwartzberg PL, Sher A, Jankovic D. The major component in schistosome eggs responsible

for conditioning dendritic cells for Th2 polarization is a T2 ribonuclease (omega-1). J Exp Med 2009; 206:1681-90.

143. Kübler E, Oesch B, Raeber AJ. Diagnosis of prion diseases. Br Med Bull 2003; 66:267-79.

144. Llorens F, Kruse N, Schmitz M, Shafiq M, da Cunha JE, Gotzman N, Zafar S, Thune K, de Oliveira JR, Mollenhauer B, et al. Quantification of CSF biomarkers using an electrochemiluminescence-based detection system in the differential diagnosis of AD and sCJD. J Neurol 2015.

145. Leitão MJ, Baldeiras I, Almeida MR, Ribeiro MH, Santos AC, Ribeiro M, Tomás J, Rocha S, Santana I, Oliveira CR. Sporadic Creutzfeldt-Jakob disease diagnostic accuracy is improved by a new CSF ELISA 14-3-3γ assay. Neuroscience 2016; 322:398-407.

Appendices

Appendix I. Cerebrospinal Fluid Protein Concentrations

Individual rats (193 dpi)	Rat ID #	Total volume collected (µl)	Protein concentration (µg/µl)
Uninfected			
	260A	175 ++	1.8
	262A	100 -B	0.5
	264B	125 -B	0.6
	267B	100 -B	0.6
	269A	150 -B	0.7
	269B	150 +	1.9
RAS			
	297A	175 ++	0.7
	297B	75 ++	2.6
	300A	100 +	0.7
	301A	100 +	0.6
	302A	150 -B	0.6
	302B	225 -B	0.6

Approximate total volume of CSF collected from individual rats was reported and samples were qualitatively scored for blood contamination (according to Table 2-1), and assessed for relative total protein concentration. These samples were used in Figure 2-2 and 2-3 and are listed in the order of loading on immunoblots for individual characterization. The symbols of +, and –B refer to blood contamination scoring as described in Chapter 2 (Table 2-1).

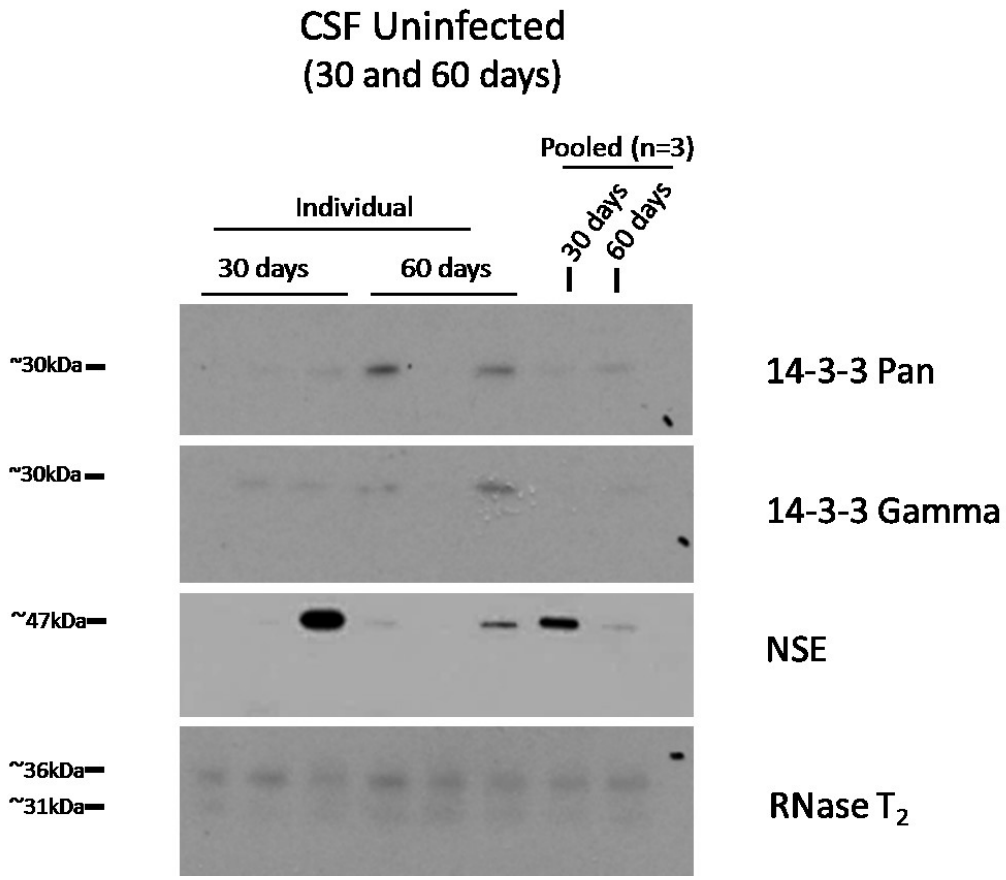

Appendix II. Protein Detection in Young Rats

Western blot analysis for 14-3-3 pan, 14-3-3 gamma, NSE, and RNase T2 of individual and pooled CSF (10 µl/well) from uninfected rats at 30 and 60 days of age. RNaseT2 is detected at low levels in CSF of young rats while 14-3-3 and NSE proteins are present at highly variable levels.

Appendix III. Statistical Analysis of Densitometry Data Collected from Western Blot Analysis

	Time Point 193 Days					
	Loaded by Volume (10µl)			Loaded by Concentration (0.4µg/µl)		
Table Analyzed	**14-3-3 pan**	**14-3-3 gamma**	**NSE**	**14-3-3 pan**	**14-3-3 gamma**	**NSE**
Column A	Control	Control	Control	Control	Control	Control
vs	vs	vs	vs	vs	vs	vs
Column B	RAS	RAS	RAS	RAS	RAS	RAS
Unpaired t test						
P value	0.1716	0.1497	0.6613	0.0213	0.0078	0.9258
P value summary	ns	ns	ns	*	**	ns
Are means signif. different? (P < 0.05)	No	No	No	Yes	Yes	No
One- or two-tailed P value?	Two-tailed	Two-tailed	Two-tailed	Two-tailed	Two-tailed	Two-tailed
t, df	t=1.473 df=10	t=1.561 df=10	t=0.4515 df=10	t=2.727 df=10	t=3.319 df=10	t=0.09545 df=10
How big is the difference?						
Mean ± SEM of column A	58730 ± 50790 N=6	156300 ± 101300 N=6	145200 ± 91970 N=6	3273 ± 1692 N=6	7440 ± 2527 N=6	101800 ± 82190 N=6
Mean ± SEM of column B	150100 ± 35610 N=6	344300 ± 65280 N=6	101400 ± 30830 N=6	167700 ± 60260 N=6	60620 ± 15820 N=6	110300 ± 34040 N=6
Difference between means	-91330 ± 62020	-188000 ± 120500	43790 ± 97000	-164400 ± 60290	-53190 ± 16020	-8491 ± 88960
95% confidence interval	-229500 to 46860	-456400 to 80410	-172300 to 259900	-298700 to -30090	-88880 to -17490	-206700 to 189700
R squared	0.1782	0.1958	0.01998	0.4265	0.5242	0.0009102
F test to compare variances						
F,DFn, Dfd	2.035, 5, 5	2.406, 5, 5	8.898, 5, 5	1268, 5, 5	39.20, 5, 5	5.829, 5, 5
P value	0.4543	0.3574	0.0315	P<0.0001	0.001	0.0756
P value summary	ns	ns	*	***	**	ns
Are variances significantly different?	No	No	Yes	Yes	Yes	No
Area under the ROC curve						
Area	0.8333	0.8056	0.6111	0.9861	0.9722	0.75
Std. Error	0.1521	0.1531	0.1879	0.02749	0.04268	0.1586
95% confidence interval	0.5351 to 1.132	0.5055 to 1.106	0.2427 to 0.9796	0.9322 to 1.040	0.8885 to 1.056	0.4392 to 1.061
P value	0.05472	0.07823	0.5219	0.005094	0.006508	0.1496

	Time Point 148 Days					
	Loaded by Volume (10µl)			Loaded by Concentration (0.4µg/µl)		
Table Analyzed	**14-3-3 Pan**	**14-3-3 Gamma**	**NSE**	**14-3-3 Pan**	**14-3-3 Gamma**	**NSE**
Column A	Control	Control	Control	Control	Control	Control
vs	vs	vs	vs	vs	vs	vs
Column B	RAS	RAS	RAS	RAS	RAS	RAS
Unpaired t test						
P value	0.5688	0.442	0.4221	0.874	0.567	0.501
P value summary	ns	ns	ns	ns	ns	ns
Are means signif. different? (P < 0.05)	No	No	No	No	No	No
One- or two-tailed P value?	Two-tailed	Two-tailed	Two-tailed	Two-tailed	Two-tailed	Two-tailed
t, df	t=0.5892 df=10	t=0.8006 df=10	t=0.8371 df=10	t=0.1627 df=10	t=0.5920 df=10	t=0.6981 df=10
How big is the difference?						
Mean ± SEM of column A	34100 ± 7555 N=6	19130 ± 5861 N=6	59980 ± 35430 N=6	47490 ± 37900 N=6	23700 ± 13730 N=6	73140 ± 62960 N=6
Mean ± SEM of column B	51250 ± 28120 N=6	27570 ± 8767 N=6	26650 ± 18170 N=6	41160 ± 8650 N=6	35030 ± 13340 N=6	153800 ± 96920 N=6
Difference between means	-17150 ± 29120	-8443 ± 10550	33330 ± 39820	6324 ± 38880	-11330 ± 19140	-80690 ± 115600
95% confidence interval	-82020 to 47710	-31940 to 15050	-55380 to 122000	-80290 to 92940	-53980 to 31320	-338200 to 176800
R squared	0.03355	0.06023	0.06548	0.002639	0.03386	0.04647
F test to compare variances						
F,DFn, Dfd	13.85, 5, 5	2.237, 5, 5	3.801, 5, 5	19.20, 5, 5	1.059, 5, 5	2.370, 5, 5
P value	0.0119	0.3975	0.1691	0.0056	0.9516	0.3655
P value summary	*	ns	ns	**	ns	ns
Are variances significantly different?	Yes	No	No	Yes	No	No
Area under the ROC curve						
Area	0.5833	0.6111	0.6944	0.7778	0.5833	0.7778
Std. Error	0.1855	0.1737	0.1698	0.1566	0.1784	0.1437
95% confidence interval	0.2197 to 0.9469	0.2705 to 0.9517	0.3616 to 1.027	0.4708 to 1.085	0.2336 to 0.9331	0.4960 to 1.060
P value	0.631	0.5219	0.2624	0.1094	0.631	0.1094

	Ribonuclease T2		
Table Analyzed	**Loaded by Volume (10µl, 193 dpi)**	**Loaded by Concentration (0.4µg/µl, 193 dpi)**	**Loaded by Volume (10µl, 148 dpi)**
Column A	Control	Control	Control
vs	vs	vs	vs
Column B	RAS	RAS	RAS
Unpaired t test			
P value	0.1716	0.1497	0.6613
P value summary	ns	ns	ns
Are means signif. different? (P < 0.05)	No	No	No
One- or two-tailed P value?	Two-tailed	Two-tailed	Two-tailed
t, df	t=1.473 df=10	t=1.561 df=10	t=0.4515 df=10
How big is the difference?			
Mean ± SEM of column A	58730 ± 50790 N=6	156300 ± 101300 N=6	145200 ± 91970 N=6
Mean ± SEM of column B	150100 ± 35610 N=6	344300 ± 65280 N=6	101400 ± 30830 N=6
Difference between means	-91330 ± 62020	-188000 ± 120500	43790 ± 97000
95% confidence interval	-229500 to 46860	-456400 to 80410	-172300 to 259900
R squared	0.1782	0.1958	0.01998
F test to compare variances			
F,DFn, Dfd	2.035, 5, 5	2.406, 5, 5	8.898, 5, 5
P value	0.4543	0.3574	0.0315
P value summary	ns	ns	*
Are variances significantly different?	No	No	Yes
Area under the ROC curve			
Area	0.8333	0.8056	0.6111
Std. Error	0.1521	0.1531	0.1879
95% confidence interval	0.5351 to 1.132	0.5055 to 1.106	0.2427 to 0.9796
P value	0.05472	0.07823	0.5219